A simple load transfer method for energy pile groups

Huaibo Song, Huafu Pei, Jean-Michel Pereira, Anh Minh A.M. Tang, Chao Zhou

A simple load transfer method for energy pile groups

Huaibo Song[1], Huafu Pei[2*], Jean-Michel Pereira[3], Anh Minh Tang[4], Chao Zhou[5]

[1] Ph.D. student, MSc, School of Civil Engineering, State Key Laboratory of Coastal and Offshore Engineering, Dalian University of Technology, Dalian, China; Navier, Ecole des Ponts, Univ Gustave Eiffel, CNRS, Marne-la-Vallée, France, E-mail: songhuaibo@mail.dlut.edu.cn; huaibo.song@.enpc.fr, https://orcid.org/0000-0002-4592-9521

[2*] Professor, Ph.D., School of Civil Engineering, State Key Laboratory of Coastal and Offshore Engineering, Dalian University of Technology, Dalian, China (corresponding author). E-mail: huafupei@dlut.edu.cn, https://orcid.org/0000-0003-3862-0865

[3] Professor, Ph.D., Navier, Ecole des Ponts, Univ Gustave Eiffel, CNRS, Marne-la-Vallée, France, E-mail: jean-michel.pereira@enpc.fr, https://orcid.org/0000-0002-0290-5191

[4] Research Director, Ph.D., Navier, Ecole des Ponts, Univ Gustave Eiffel, CNRS, Marne-la-Vallée, France, E-mail: anh-minh.tang@enpc.fr, https://orcid.org/0000-0002-7149-8497

[5] Associate Professor, Ph.D., Department of Civil and Environmental Engineering, The Hong Kong Polytechnic University, Hung Hom, Kowloon, HKSAR, China, E-mail: zhou@polyu.edu.hk

Abstract

Various analysis methods have been developed to simulate the performance of energy pile groups subjected to thermal and mechanical loads. Although they considered the interactions between piles in the group, the 'sheltering-reinforcing' effect was usually ignored during the analysis, or the methods were not experimentally validated. Therefore, to address this gap, we propose an experimentally validated load transfer model that considers the 'sheltering-reinforcing' effect for the thermomechanical analysis of energy pile groups. The proposed method modeled two well-documented full-scale field tests and two finite-element simulation cases. The comparison results showed that the proposed method could capture several essential aspects of the energy pile group, including thermally induced strain, stress, displacement, and group effects. Furthermore, a parametric analysis was performed to evaluate the effects of relevant parameters on the thermomechanical behavior of the energy pile group.

Keywords: load transfer method; energy pile group; thermomechanical behavior; geothermal energy.

1. Introduction

Energy piles are environment-friendly technologies that have attracted increasing attention

because of their effective solicitation of shallow geothermal energy (Rotta Loria and Coulibaly 2021). Unlike conventional pile foundations, the operation of an energy pile involves complex coupling between thermal, mechanical, and other physical fields (Bourne-Webb and Bodas Freitas 2020). It is also necessary to consider pile–pile and pile-slab interactions under thermal-mechanical loading for energy pile groups (Moradshahi et al. 2020, Ravera et al. 2020a, 2020b, Fang et al. 2022). Recently, understanding this complex mechanism, seeking simple approaches to describe it, and then applying it to the engineering design of energy piles has become a hot topic in energy pile research.

Numerous in situ field tests (Bourne-Webb et al. 2009, Murphy et al. 2015, Faizal et al. 2019, Sutman et al. 2019a, Fang et al. 2020, 2022, Wu et al. 2020, 2021), small-scale laboratory model tests (Kalantidou et al. 2012, Yavari et al. 2016a, Yazdani et al. 2019b, Kong et al. 2020, Song et al. 2020), and centrifuge model tests (Ng et al. 2015, 2016, 2021, Ng and Ma 2019) have been conducted to investigate the thermomechanical behavior of energy pile and pile groups. It is impractical to use experimental methods to comprehensively investigate the effects of all the factors on the performance of energy piles considering the enormous time-consuming and financial expense. Thus, the development of experimentally verified numerical methods to supplement the experimental methods is necessary to thoroughly study the thermomechanical mechanisms of energy piles. Various numerical approaches with different complexities have been used in previous years, including finite element models (Yavari et al. 2014, Rammal et al. 2018, Garbellini and Laloui 2019a, Nguyen et al. 2019, Arzanfudi et al. 2020, Georgiadis et al. 2020, Sutman et al. 2020), finite difference models (Suryatriyastuti et al. 2012, 2014, Luo and Hu 2019, Najma and Sharma 2021, Liu et al. 2022), and other theoretical models (Rotta Loria and Laloui 2016, 2017a, Rotta Loria et al. 2018, 2020a, Garbellini and Laloui 2019a, Iodice et al. 2020, 2023, Ravera et al. 2020a, 2020b, Cui et al. 2021, Saeidi Rashk Olia et al. 2022, Liu et al. 2022, Song et al. 2022, Song and Pei 2022, Pei et al. 2022a). Among these, the load transfer method is commonly used for energy pile design because it overcomes the drawbacks of high time consumption, high computational cost, and high requirements of the complete

numerical simulation method. The load transfer method is very user-friendly and well-suited for the engineering design of energy piles.

The load transfer method was initially proposed by Seed and Reese (Seed and Reese 1957) and then gradually applied to investigate the thermomechanical response of an isolated energy pile. For example, Knellwolf et al. (2011) developed a load transfer method using the three-polyline load transfer curve proposed by Frank and Zhao (1982). In situ isolated energy piles were modeled, and their thermomechanical behavior was analyzed. The comparison results between the simulations and the measured data showed good agreement. Sutman et al. (2019b) developed a model by incorporating the unloading-reloading response into the load transfer curve and validated it through field test results. The above studies demonstrate the applicability of the load transfer method for studying the thermomechanical response of an isolated energy pile. As an essential part of the energy pile group, the successful application of the single pile response model lays the foundation for developing a pile group response model.

Recently, several studies (Ravera et al. 2020a, Fei et al. 2022, Liu et al. 2022) extended the load-transfer method to consider the thermomechanical interaction of energy piles in groups. Ravera et al. (2020a) modified the load transfer curve of an isolated energy pile in a group using a displacement factor that considered group effects. The field test results of an energy pile group consisting of four energy piles were used to validate the proposed method. A comparison between the simulated and measured results showed the suitability of the proposed method for analyzing the thermomechanical performance of the energy pile group. Nevertheless, it should be noted that the determination of the displacement factor is based on an empirical formula, which is proposed based on the fitting of the finite-difference modeling results of the 5×5 pile group (Comodromos et al. 2016). A significant difficulty in applying this empirical formula to the analysis of the energy pile group is that the effect of the temperature on displacement factor cannot be considered. Thus, additional experiments or numerical simulations are required for specific analysis cases to comprehensively determine the appropriate displacement factors. Besides, the load transfer method proposed by Ravera et al. (2020a) has some limitations in

87 clarifying the thermomechanical behavior of energy pile groups because it cannot take into
88 account the 'sheltering-reinforcing' effects of the energy pile group into consideration.
89 The 'sheltering-reinforcing' effects characterize the interaction between piles in groups and
90 are considered in previous studies of conventional pile groups (Mylonakis and Gazetas 1998,
91 Wang et al. 2016). The results indicated that the calculated pile head displacement was
92 overestimated without considering this effect, and the error increased significantly with
93 increasing group size. For the energy pile group, the 'sheltering-reinforcing' effects act
94 throughout thermomechanical loading, which can be observed in the field test results (Rotta
95 Loria and Laloui 2017b, 2018, Fang et al. 2020). Liu et al.(2022) proposed a load transfer
96 method to rapidly calculate the response of an energy pile group in which they considered the
97 reinforcing effect of neighboring piles in the group. The applicability of this method to pile
98 groups was verified by comparing it with finite element simulations that did not consider the
99 nonlinear pile-soil interaction (Rotta Loria and Laloui 2016). Nevertheless, the presence of the
100 slab and the pile-slab-soil interaction had not been considered in their study, which would limit
101 the scope of application of the method due to the importance of the slab in the energy pile group.
102 Besides, there is no adequate verification of whether the proposed model can accurately
103 calculate the critical aspects of the thermomechanical responses of the energy pile group,
104 including the pile axial strain, stress, and pile head displacement. Therefore, to address this gap,
105 it is necessary to develop an experimentally validated model.
106 This study aims to provide an experimentally validated simple load transfer model that
107 considers the 'sheltering-reinforcing' effects for thermomechanical analysis of energy pile
108 groups. Section 2 details the proposed model and the developed thermomechanical performance
109 analysis algorithm for energy pile groups based on the proposed model. Section 3 verifies the
110 results obtained by the proposed method using field tests and finite element simulations. A
111 comprehensive sensitivity analysis of the parameters involved in the proposed model is
112 presented in Section 4. Finally, conclusions are presented in Section 5.

2. Development of the load transfer model for the energy pile group

Some assumptions of the load transfer mechanism for energy piles are employed in this study: (1) the load-displacement relationship (i.e., t-z model) and pile and soil properties are assumed to be independent of temperature variations, based on the fact that previous studies suggested that the effect of temperature within the range of 5 - 40 ℃ on soil and concrete properties is insignificant (Yavari et al. 2016b, Yazdani et al. 2019a, Rotta Loria and Coulibaly 2021); (2) the strain and stress analysis of the energy pile in the group is achieved by considering the pile-to-pile interaction in the pile group; (3) the interaction between the slab, energy piles in the group, and soil can be considered through assuming an additional spring connecting with the pile heads; (4) The influence of the axial deformation of the piles on the thermomechanical behavior of the piles is mainly considered in the study to simplify the calculation(Ravera et al. 2020a). The last assumption is based on the fact that a numerical study of energy piles (Olgun et al. 2014) and full-scale field studies (Faizal et al. 2019) reported that the normal contact stress of the piles did not change significantly owing to their radial thermal expansion of the energy piles. Other studies on the load transfer analysis (Knellwolf et al. 2011; Chen and McCartney 2016) have also confirmed that the influence of radial deformation on the pile-soil axial interaction is negligible. Therefore, the present study did not consider the influence of the radial deformation of the energy pile.

2.1 Load transfer function at the shaft of the isolated energy pile

According to a previous study (Lee and Xiao 2001), the nonlinear performance of the pile load displacement is divided into (i) the nonlinear relationship between the pile shaft shear stress and pile-soil relative displacement and (ii) the nonlinear stress-strain relationship of the surrounding soil induced by the pile shaft shear stress. Caputo (1984) and Trochanis et al. (1991) divided surrounding soil into disturbed and undisturbed zones. The disturbed zone is a thin layer of soil on the soil/pile interface. The nonlinearity of the pile-soil interaction was concentrated in this interface. The area outside the interface is the undisturbed zone. Because this zone is subjected to a relatively low stress change, the stress-strain behavior of the soil is

mainly elastic. The nonlinear response of pile groups primarily depends on the nonlinear characteristics of single piles, and the pile-pile interaction is elastic. The total shaft displacement at a certain depth (i.e., u) can be divided into pile-soil relative displacement (i.e., p) and the elastic displacement of the surrounding soil (i.e., s).Recently, these concept has been introduced into the thermomechanical analysis of energy pile group (Fei et al. 2020, Liu et al. 2022). As suggested by Lee and Xiao (2001), the thickness of the interface was assumed to be zero, which can provide a simplified mathematical processing method for simulating the pile-soil relative displacement and elastic displacement of the soil around the pile. Thus, the total pile shaft displacement can be expressed as follows:

$$u = p + s \tag{1}$$

The elastic soil displacement induced by pile shaft stress can be calculated using the expression proposed by Randolph and Worth (1978):

$$s = \frac{\tau r_0}{G} \ln \frac{r_m}{r_0} = \psi \tau \tag{2}$$

where G is the shear modulus of the soil, r_0 is the pile radius, r_m is the shear influence radius.

In this study, an exponential model was employed to calculate the pile-soil relative displacement of the pile-soil interface because it can better simulate the field test results without adopting complex fitting parameters (Kezdi. 1957). The exponential model is expressed as follows:

$$\tau = \tau_u \left[1 - \exp\left(-\frac{G_{s\max}}{\tau_u} p \right) \right] \tag{3}$$

where τ is the pile shaft shear stress, τ_u is the ultimate shear stress, $G_{s,max}$ is the initial stiffness of the pile-soil interface, the unit of which is kPa/m.

It should be noted that the deformation mechanisms of energy piles and conventional piles differ. For the energy pile, when the pile body is heated up, it expands, the upper part of the pile side friction decreases, and it is in the unloading stage. In contrast, the shaft shear stress at the

lower end of the pile side increases and is in a loading state. When the pile body is cooled, it shrinks, and the situation is the opposite of that during heating. Therefore, Eq. (3) should be improved for the thermomechanical analysis of the energy pile. We developed a model by employing the improved Masing rule to simulate the loading-unloading-reloading path of the pile-soil interaction, and its expression can be written as Eq. (4). Further details can be found in (Pei et al. 2022b).

$$\tau = \tau_0 + \eta\left(\tau_u - \eta\tau_0\right)\left[1 - \exp\left(-\eta\frac{G_{s,\max}}{\tau_u - \eta\tau_0}\left(p - p_0\right)\right)\right] \tag{4}$$

where η denotes the loading and unloading branching judgment factor, $\eta = -1$ and $\eta = 1$ represent unloading and reloading conditions, respectively, p_0 denotes the relative displacement of the pile and soil corresponding to the stress reverse point, τ_0 is the pile shaft stress corresponding to the stress reversal point. When p_0 and τ_0 are equal to zero, Eq.(4) degenerates to the expression of the initial loading curve.

Substituting Eqs. (2) and (4) into Eq. (1), the total pile shaft displacement at a given depth can be expressed as Eq. (5):

$$u = p + s = p_0 + \frac{\eta\tau_0 - \tau_u}{\eta G_{s\max}}\ln\left(1 - \frac{\tau - \tau_0}{\eta\left(\tau_u - \eta\tau_0\right)}\right) + \psi\tau \tag{5}$$

where $p_0 = u_0 - s_0 = u_0 - \psi\tau_0$, and u_0 denotes the total shaft displacement of the pile corresponding to the shaft shear stress reversal point. Thus, Eq. (5) can be expressed using Eq. (4), which is the load transfer function used to simulate the relationship between the pile shaft resistance and the relative pile-soil displacement.

$$u = u_0 + \frac{\eta\tau_0 - \tau_u}{\eta G_{s\max}}\ln\left(1 - \frac{\tau - \tau_0}{\eta\left(\tau_u - \eta\tau_0\right)}\right) + \psi\left(\tau - \tau_0\right) \tag{6}$$

2.2 Group interaction for energy piles considering 'sheltering-reinforcing' effect

As discussed in the previous section, the pile-soil-pile interaction in the pile group can be considered as linearly elastic and suitable for the principle of superposition. According to previous studies (Randolph and Wroth 1979), for the two energy piles system (i and j)

subjected to thermomechanical loading, the vertical elastic displacement of the pile i can be divided into three parts: (i) the displacement (s_{i0}) induced by its own load; (ii) the displacement (Δs_{i0}) induced by the 'sheltering-reinforcing' effect of pile j; (iii) the additional displacement (s_{ij}) caused by j pile under its own load. If the 'sheltering-reinforcing' effect is not considered, the total elastic displacement of i pile can be written as follows:

$$s_i = s_{i0} + s_{ij} \tag{7}$$

In the proposed method, we consider the 'sheltering-reinforcing' effect. Therefore, the total elastic displacement of i pile can be written as follows:

$$s_i = s_{i0} - \Delta s_{i0} + s_{ij} \tag{8}$$

According to the formulation proposed by Randolph and Worth (1978), s_{i0} can be calculated as follows:

$$s_{i0} = \frac{\tau_{si} r_0}{G} \ln \frac{r_m}{r_0} \tag{9}$$

The shear stress of pile i transferred to the side of pile j can be expressed as follows:

$$\tau_{sji} = \frac{\tau_{sij} r_0}{s_{aij}}, (r_0 < s_{aij} < r_m) \tag{10}$$

where s_{aij} denotes the distance between the axes of two piles. Considering the 'sheltering-reinforcing' effects of pile j on pile i, Δs_{i0} can be obtained by:

$$\Delta s_{i0} = \frac{\tau_{sji} r_0}{G} \ln \frac{r_m}{s_{aij}} = \frac{\tau_{sij} r_0}{s_{aij}} \frac{r_0}{G} \ln \frac{r_m}{s_{aij}} \tag{11}$$

If the existence of pile j is not considered, then the displacement at the position of pile j caused by pile i under its own load is:

$$s_{ji0} = \frac{\tau_{sji} r_0}{G} \ln \frac{r_m}{s_{aij}}, (r_0 < s_{aij} < r_m) \tag{12}$$

In addition, the shear stress transferred from pile i to the side of pile j (i.e., τ_{sij}) reduces the displacement of pile j as follows:

$$\Delta s_{ji0}=\frac{\tau_{sji}r_0}{G}\ln\frac{r_m}{r_0}=\frac{\tau_{sji}r_0}{s_{aij}}\frac{r_0}{G}\ln\frac{r_m}{r_0} \tag{13}$$

Therefore, the additional displacement of pile j induced by the load of pile i can be expressed as follows:

$$s_{ji}=s_{ji0}-\Delta s_{ji0}=\frac{\tau_{sji}r_0}{G}\left(\ln\frac{r_m}{s_{aij}}-\frac{r_0}{s_{aij}}\ln\frac{r_m}{r_0}\right) \tag{14}$$

According to the assumption that $\tau_{sij}=\tau_{sji}=\tau_{si}$ (Zhang et al. 2016), the additional elastic displacement of pile i caused by the load of pile j is equal to the additional elastic displacement of pile j caused by the load of pile i, that is:

$$s_{ij}=s_{ji}=\frac{\tau_{si}r_0}{G}\left(\ln\frac{r_m}{s_{aij}}-\frac{r_0}{s_{aij}}\ln\frac{r_m}{r_0}\right) \tag{15}$$

Thus, for a two-pile system, the total elastic displacement of pile i can be obtained as follows:

$$s_i=s_{i0}-\Delta s_{i0}+s_{ij}=\frac{\tau_{si}r_0}{G}\left[\ln\frac{r_m}{r_0}-\frac{r_0}{s_{aij}}\ln\frac{r_m}{s_{aij}}+\ln\frac{r_m}{s_{aij}}-\frac{r_0}{s_{aij}}\ln\frac{r_m}{r_0}\right] \tag{16}$$

For a group of n piles, the total elastic displacement of pile i can be calculated as follows:

$$s_i=s_{i0}-\sum_{j=1,j\neq i}^{n}\left(\Delta s_{i0}-s_{ij}\right)=\frac{\tau_{si}r_0}{G}\left[\ln\frac{r_m}{r_0}-\sum_{j=1,j\neq i}^{n}\left(\frac{r_0}{s_{aij}}\ln\frac{r_m}{s_{aij}}-\ln\frac{r_m}{s_{aij}}+\frac{r_0}{s_{aij}}\ln\frac{r_m}{r_0}\right)\right] \tag{17}$$

Therefore, the total shaft displacement of the energy pile i is:

$$u=p+s=u_0+\frac{\eta\tau_0-\tau_u}{\eta G_{s\max}}\ln\left(1-\frac{\tau_{si}-\tau_0}{\eta\left(\tau_u-\eta\tau_0\right)}\right)+\psi'\left(\tau_{si}-\tau_0\right) \tag{18}$$

where ψ' is the pile-pile interaction parameter, which can be written as follows:

$$\psi'=\frac{r_0}{G}\left[\ln\frac{r_m}{r_0}-\sum_{j=1,j\neq i}^{n}\left(\frac{r_0}{s_{aij}}\ln\frac{r_m}{s_{aij}}-\ln\frac{r_m}{s_{aij}}+\frac{r_0}{s_{aij}}\ln\frac{r_m}{r_0}\right)\right] \tag{19}$$

2.3 Load transfer function at the base of energy pile group

Similar to the definition of the pile-side displacement, the displacement at the pile end is the sum of the pile-soil relative displacement (i.e., p_p) and the elastic displacement of the soil at the pile tip (i.e., s_p). It can be written as

$$u_p = p_p + s_p \tag{20}$$

The pile-soil relative displacement can be simulated using an exponential model (Liu et al., 2022), which can be calculated as follows:

$$\sigma_p = \sigma_{up}\left[1-\exp\left(-\frac{G_{p\max}}{\sigma_{up}}p_p\right)\right] \tag{21}$$

where σ_p is the pile tip resistance, G_{pmax} is the initial stiffness of the pile tip-soil interface; σ_{up} is the ultimate pile tip resistance.

According to the improved Masing rule (Pei et al. 2022), the load transfer function for simulate the loading-unloading-reloading path of the pile-soil interaction at the pile tip can be written as

$$\sigma_p = \sigma_{p0} + \kappa\left(\sigma_{up} - \eta\sigma_{p0}\right)\left[1-\exp\left(-\kappa\frac{G_{p\max}}{\sigma_{up}-\kappa\sigma_{p0}}\left(p_p - p_{p0}\right)\right)\right] \tag{22}$$

Thus, the pile-soil relative displacement of the energy pile tip can be written as

$$p_p = p_{p0} + \frac{\kappa\sigma_{p0}-\sigma_{pu}}{\kappa G_{p\max}}\ln\left(1-\frac{\sigma_p-\sigma_{p0}}{\kappa\left(\sigma_{pu}-\kappa\sigma_{p0}\right)}\right) \tag{23}$$

where κ denotes the loading and unloading branching judgment factor, $\kappa=-1$ and $\kappa=1$ represent unloading and reloading conditions, respectively, p_{p0} denotes the relative displacement of the pile tip and soil corresponding to the stress reversal point, σ_{p0} is the pile tip resistance corresponding to the stress reversal point. When p_{p0} and σ_{p0} equal zero, Eq. (22) degenerates to the expression for the initial loading curve.

According to Randolph and Wroth (1979), the elastic vertical displacement of the soil induced by the pile tip resistance can be obtained as

$$s_p = \frac{\pi r_0 (1-\nu)}{4G_{soil}} \sigma_p = \lambda \sigma_p \tag{24}$$

where λ is the model parameter. According to the studies in (Lin and Dai 2014), the pile-pile interaction at the pile tip is insignificant. Therefore, the total displacement of the pile tip can be expressed as follows:

$$u_p = p_p + s_p = p_{p0} + \frac{\eta\sigma_{p0} - \sigma_{pu}}{\eta G_{p\max}} \ln\left(1 - \frac{\sigma_p - \sigma_{p0}}{\eta\left(\sigma_{pu} - \eta\sigma_{p0}\right)}\right) + \lambda\sigma_p \tag{25}$$

where $p_{p0} = u_{p0} - s_{p0} = u_{p0} - \lambda\sigma_{p0}$, and u_{p0} denotes the total displacement of the pile tip corresponding to the pile tip resistance reversal point. Thus, Eq.(25) can be expressed as Eq.(26), which is the load-transfer function used to simulate the relationship between the pile tip resistance and the relative pile tip-soil displacement.

$$u_p = u_{p0} + \frac{\eta\sigma_{p0} - \sigma_{pu}}{\eta G_{p\max}} \ln\left(1 - \frac{\sigma_p - \sigma_{p0}}{\eta\left(\sigma_{pu} - \eta\sigma_{p0}\right)}\right) + \lambda\left(\sigma_p - \sigma_{p0}\right) \tag{26}$$

2.4 Pile-slab-soil interaction for the energy pile group

The pile-slab-soil interaction of the energy pile group is simulated using a spring linked to the pile head during the load transfer method, as adopted by Knellwolf et al. (2011) and Ravera et al. (2020a). The spring stiffness is calculated by (Randolph 1994, Selvadurai 2013)

$$k_h = \frac{E_s \sqrt{B_{slab} L_{slab}}}{\left(1 - \upsilon_s^2\right)\rho_0} \tag{27}$$

where E_s is Young's modulus of the soil; ν_s is Poisson's ratio of the ssoil; L_{slab} and B_{slab} are the length and width of the slab, respectively; and ρ_0 is a coefficient, which can be evaluated from the dimensions of the slab (Ravera et al. 2020a).

2.5 Parameters determination

As shown in Fig. 1, the proposed model has four parameters that are calculated as follows:

(1) Ultimate shaft resistance τ_u

The ultimate shear stress is the stress corresponding to the asymptote of the stress-strain

curve, which is obtained by laboratory interface shear tests. If the test data are not available, the ultimate shear stress can be calculated as follows:

$$\tau_u = (1-\sin\varphi_s)\sigma'_z \tan\delta_s \tag{28}$$

where σ'_z is the effective overburden pressure, $\sigma'_z = \gamma' z$ for the homogeneous soil and $\sigma'_z = \sum_{i=1}^{n} \gamma'_i z_i$ for the layered soil, where γ' is the effective weight of the soil. δ_s is the friction angle of the pile-soil interface, which can be expressed by the soil friction angle (φ_s) as $\delta_s = tan^{-1}\frac{sin\varphi_s cos\varphi_s}{1+sin^2\varphi_s}$ (Pei et al. 2022b).

(2) Initial stiffness of the pile-soil interface G_{smax}

According to Randolph and Worth (1978), G_{smax} can be obtained as follows:

$$G_{smax} = \frac{2G_s}{D\ln\frac{2r_m}{D}} \tag{29}$$

where G_s is the soil shear modulus and r_m is the shear influence radius, which is related to the pile length and soil layer distribution. The value of the shear influence radius increases with increasing soil depth. It can be expressed by:

$$r_m = 2\delta(1-\nu_s)L \tag{30}$$

where δ is the soil shear modulus ratio, ν_s is the Poisson's ratio of the soil, L is the pile length. For homogeneous soils, the soil shear modulus ratio can be calculated as $\delta = {}^{G_{\frac{L}{2}}}/_{G_L}$, where $G_{\frac{L}{2}}$ and G_L are the soil shear modulus at the middle and tip of the pile, respectively. For multilayered nonhomogeneous soils, the soil shear modulus ratio can be calculated as $\delta = \int G_{iz}dz/G_L L$ according to Lee et al. (1993), in which G_{iz} is the shear modulus of the soil layer and z is the soil depth. According to Wong and Teh (1995), the shear influence radius should adopt a value in the range of 0.5-2.5L when the length-to-diameter ratio of the pile falls within the range of 20-100.

(3) Ultimate base resistance σ_{up}

σ_{up} can be calculated as $\sigma_{up} = c' N_c + \sigma'_{vb} N_q$, where c' is the effective cohesion of the

soil, σ'_{vb} is the effective vertical stress at the pile tip; N_q and N_c are the load capacity coefficients, which can be calculated by $N_q = e^{\pi tan\varphi'} tan^2(\frac{\pi+2\varphi'}{4})$, $N_c = (N_q - 1)cot\varphi'$, where φ' is the effective friction angle of the pile tip soil.

(4) Initial shear stiffness of the pile tip G_{pmax}

The initial shear stiffness of the pile tip, which can be calculated as $G_{pmax} = 4G_s / \pi r_0(1-\nu_s)$.

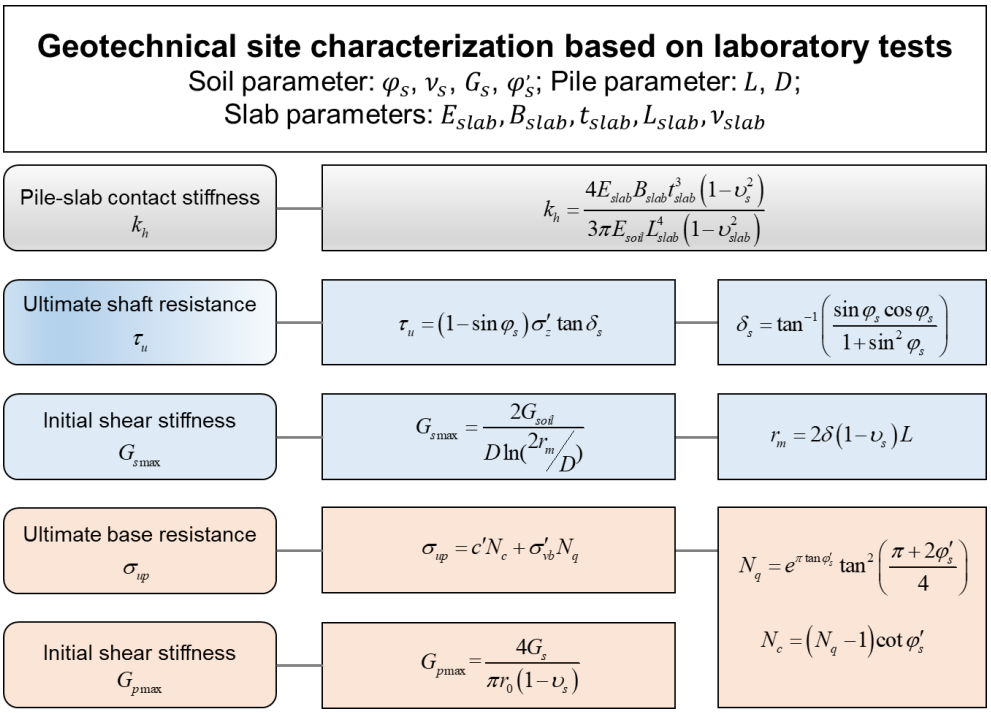

Fig. 1 Steps of calculation for the determination of model parameters

2.6 Implementation for thermomechanical analysis of an energy pile group

Approaches such as the one-dimensional element and finite difference methods can implement the proposed load transfer model. Song and Pei (2022) improved the finite-difference method proposed by Chen and McCartney (2016), which was divided into mechanical and thermomechanical analyses, as shown in Fig.2. During the mechanical analysis, the temperature change is set to zero and the pile is subjected to the mechanical load only. Besides, no constraint is applied to the pile head since the pile only moves downwards caused by the mechanical load. The mechanical response could be obtained through an iterative

procedure.

When the energy pile is subjected to heating/cooling, the pile expands or contracts, a null point (NP) is defined as the position below and above which the pile has opposite displacements. In the thermomechanical analysis stage, the position of the NP should be assumed first, and then the element number above and below the NP should be determined. The displacement calculation of the element below the NP starts from the NP+1 element. Since the displacement of NP caused by the thermal load is zero, the initial displacement of this element is the displacement under the mechanical load. Taking this as the initial element, one iteratively calculates the displacement of all pile elements below the NP and calculates the stress of each element from the pile bottom element upward based on the displacement. The displacement and stress calculation methods for elements above the NP are similar to those below the NP. The difference is that the stress is calculated sequentially from the downward pile head element. The stress at the top of the pile head element is determined by the mechanical load, restraint conditions, and element displacement. The convergence condition of each element under the thermal-mechanical coupling is that the thermal deformation tends to converge (i.e., $|\Delta_{T,new}^{i} - \Delta_{T}^{i}|<10^{-6}$). At the same time, the position of the assumed NP is adjusted by observing the stress balance of the upper and lower elements on the NP until the positions of the new and old NP reach the convergence condition and the thermomechanical response of all elements of the pile body can be obtained. It should be noted that the load transfer functions of the pile shaft resistance and tip reaction presented in Section 2 are employed during the thermomechanical analysis of the energy pile group in the present study.

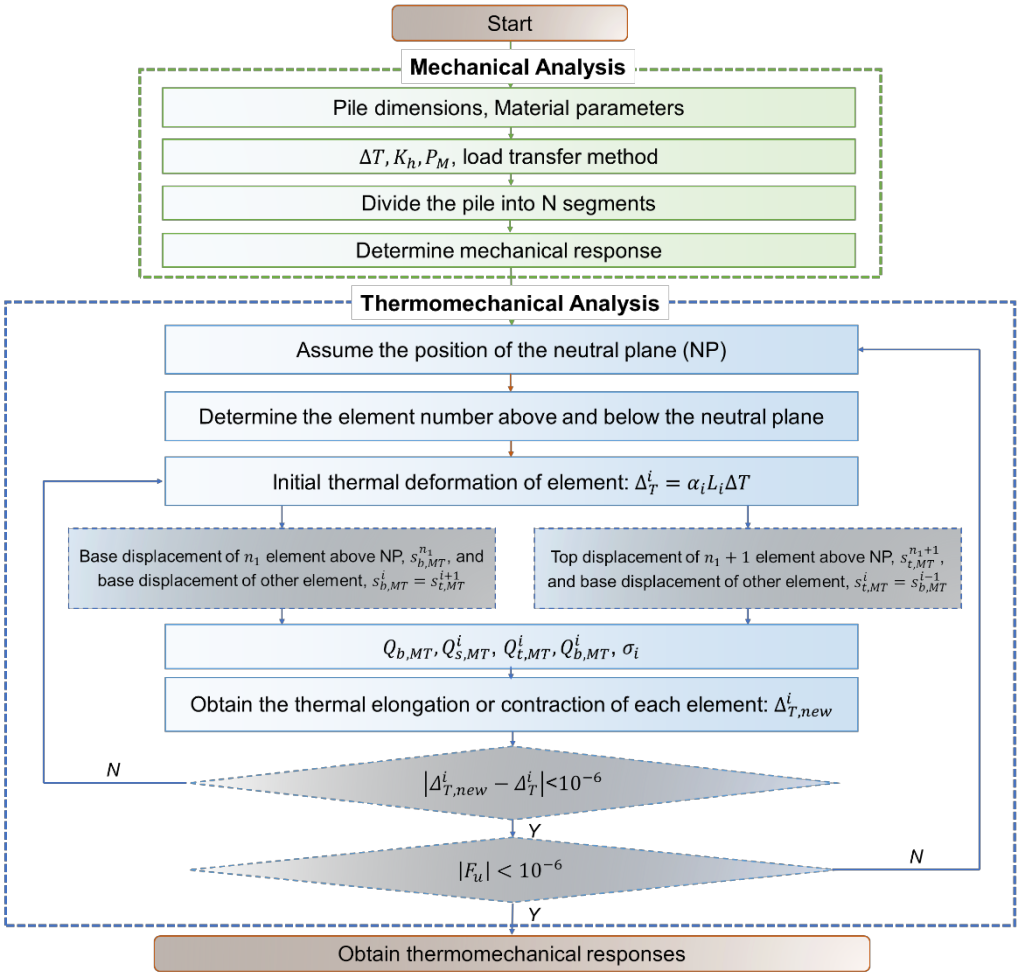

Note: ΔT=temperature change; K_h=contact stiffness; P=mechanical load; n=thermal cycles; N=number of pile elements; NP=neutral plane of the pile subjected to thermal loading; Δ_T^i=free thermal deformation of element; α_i=thermal expansion coefficient of the pile; ΔT=temperature change of the pile; $Q_{b,MT}$= pile tip reaction; $Q_{s,MT}^i$=side friction of the element subjected to thermal and mechanical loading; $Q_{t,MT}^i$=thermomechanical top axial stress of the element; $Q_{b,MT}^i$= thermomechanical base axial stress of the element; σ_i=axial stress of the element; $\Delta_{T,new}^i$=calculated thermal elongation or contraction of the element; $\sum Q_T^{NP}$=unbalanced force between the pile above and below the neutral plane.

Fig. 2 Flow chart for computational thermo-mechanical analysis of energy piles (after Song and Pei 2022)

3. Validation of the present model

3.1 Tests of an isolated energy pile

Guo et al. (2018) reported an energy pile field test conducted at Southeast University, Nanjing City, China. The groundwater of the site is located at a depth of 1m. The test pile with a length of 24 m and a diameter of 0.5 m was made of high-strength concrete. The pile was placed in five soil layers, as shown in Fig.3. The top layer of the soil deposit is clay, reaching a depth of 4.3 m. The following layers were silty clay with a thickness of 7.2 m. Below the silty

clay, two clay layers were found and reached depths of 16 and 17.4 m, respectively. The last layer is silty clay with a thickness of 6.6 m, which provides pile tip resistance. Relevant parameters for the present study were extracted from Guo et al. (2018) and are shown in Table 1. The pile was continuously heated for 168 h at an average power of 3.44 kW. In this study, the heating durations of 24, 72, 96, and 168 h are selected to be modeled, corresponding to the pile temperature variations of 11.1, 13.2, 16.6, and 19.3 ℃. No mechanical load was imposed on the pile head during testing, thus the change in pile stress was caused by the thermal load only. In addition, the contact stiffness between the pile head and superstructure was not considered in this case study because there were no structural constraints on the top of the pile.

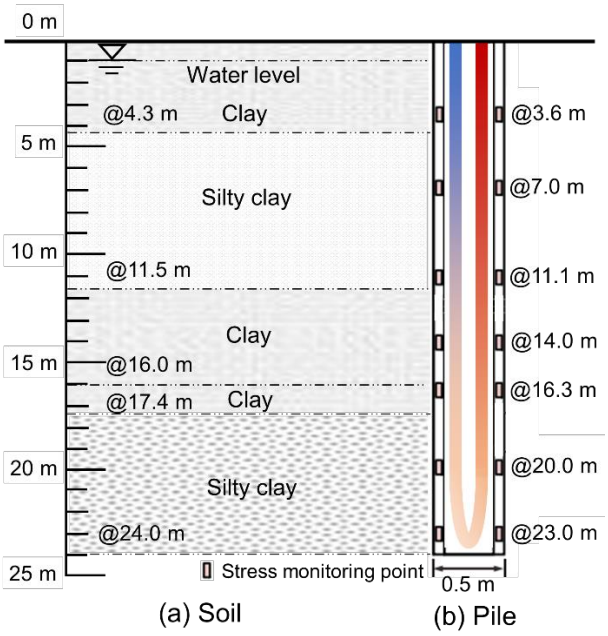

Fig. 3 Schematic of the soil and pile referring to the study of Guo et al. (2018)

Table 1 Soil parameters considered for modelling the field tests of Guo et al. (2018)

Variable \ Soil layer, z [m]	Clay [0-4.3]	Silty clay [4.3-11.5]	Clay [11.5-13.5]	Clay [13.5-16]	Silty clay [16-24]	Pile tip [24, -]	Pile
Unit weight, γ_{sat} $[kN/m^3]$	18.9	17.4	19.7	19.5	19.9	-	24.9
Ultimate skin friction, τ_u $[kPa]$	2.6	6.5	10.3	22.9	31.9		
Young's modulus, E $[MPa]$	4.6	3.6	7.5	6.6	7.3	-	45700
Shear modulus, $G_{soil}[MPa]$	17.1	13.9	28.5	25.2	15.1	-	-
Friction angle, φ [∘]	10	6.6	6.8	18.4	17.3	-	-
Initial stiffness of skin friction, $G_{max}[MPa/m]$	13.1	11.1	22.9	20.3	11.8	-	-
Ultimate tip resistance, q_b $[MPa]$	-	-	-	-	-	50	-
Initial stiffness of tip reaction,	-	-	-	-	-	1200	-

$G_{pmax}[MPa/m]$							
Thermal dilation coefficient, α_s ($\mu\varepsilon$/℃)	-	-	-	-	-	-	11.6

Fig. 4 shows the thermally induced pile axial stresses obtained from the experiments and the model used in this study. A close agreement between the measured and computed values for all the heating steps is observed. The computed thermal stress meaningfully yields a value of zero at the pile head, which reflects the absence of restraint provided by any structural elements. The thermal stress increases with the pile depth and decreases again towards the pile tip. Differences between the simulations and measurements along the pile in the first two soil layers can be found. The reason may be attributed to the significant variations of the ultimate skin friction of the first three soil layers, i.e., 37.82, 12.4 and 106.4 kPa for the first, second and third soil layers, respectively. As the temperature change increases, the second layer of soil needs to mobilize more friction than under lower temperature changes to resist the significantly increased relative pile-soil displacement. Even the third soil layer may mobilize more friction when the second soil layer is incapable of providing enough friction to reach the limit equilibrium, which would induce the stress redistribution along the pile depth and thus explains the variation of the thermal stress of the pile body in the second layer of soil. A similar phenomenon can also be found in previous studies (Rotta Loria and Laloui 2018, Fang et al. 2020).

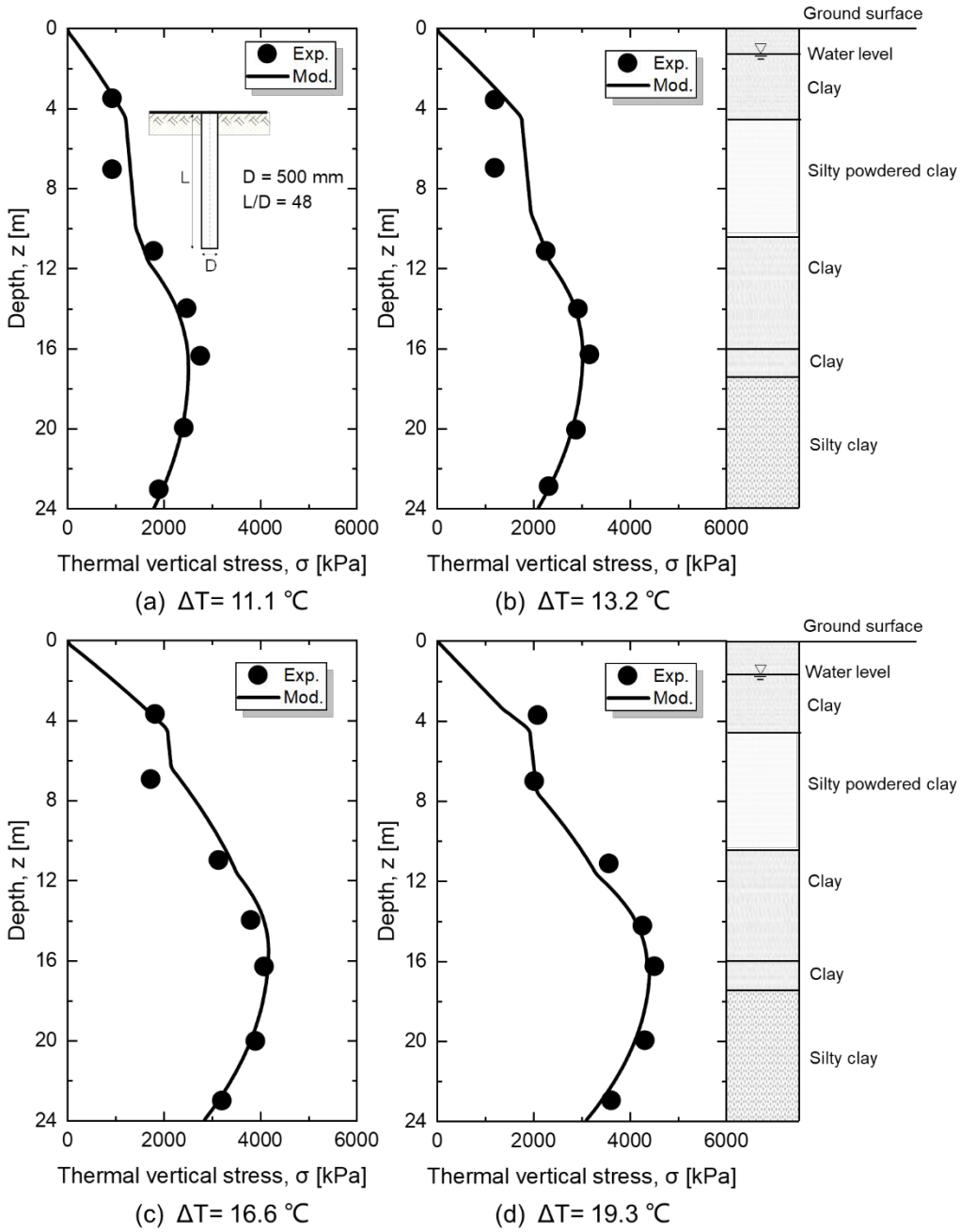

Fig. 4 Experimental and modeled thermally induced pile axial stresses referring to the tests of Guo et al. (2018). (a) ΔT=11.1 ℃; (b) ΔT=13.2 ℃; (c) ΔT=16.6 ℃; (d) ΔT=19.3 ℃

Fig. 5 shows the measured and modeled thermal stress at different pile depths versus the average temperature variations of the pile. The computed results capture the overall evolution of the measurements. It can be seen that the computed thermal stress at each depth along the pile has an approximately linear relationship with the temperature change. The maximum thermal stress is at a depth of about 16.3m. The relationship with the average temperature change is $\sigma = 236\Delta T$ kPa.

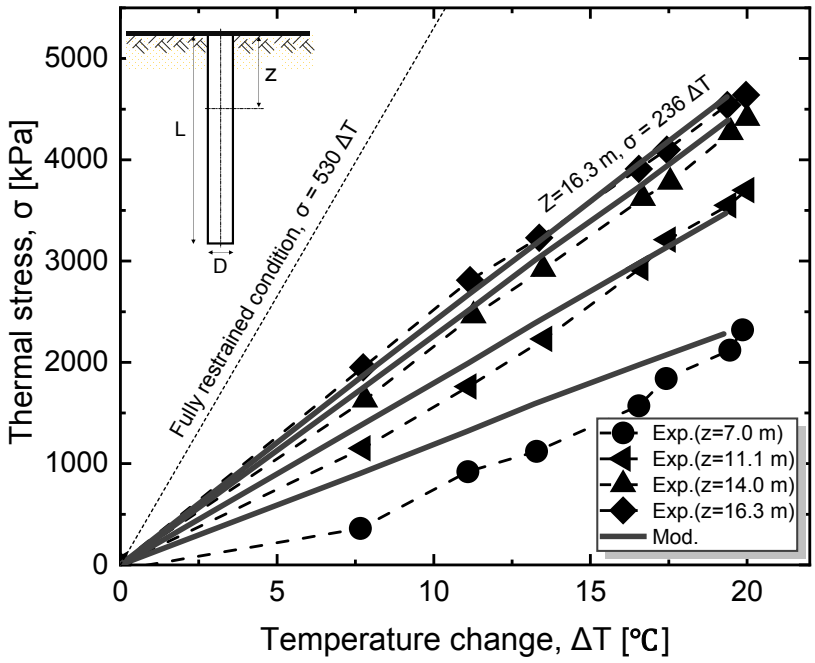

Fig. 5 Experimental and modeled thermal stresses at the different pile depths during thermal loading referring to Guo et al.(2018)

3.2 Tests of an energy pile group

The analysis case was a full-scale field test of a pile group consisting of four energy piles, as reported by Mimouni and Laloui (2015) and Rotta Loria and Laloui (2017, 2018). The energy piles (EP) have a diameter of 0.9 m and a length of 28 m; their arrangement is shown in Fig. 6a. The pile group joint has a slab of 26 m long, 0.9 m thick, and 10 m wide. The piles were placed in five soil layers as shown in Fig 6b. The top layer of the soil deposit was alluvial, reaching a depth of 8.6 m. The subsequent layer is a sandy–gravelly moraine with a thickness of 8 m. Below it, a thin bottom moraine layer is found and reaches a depth of 20.1 m. The last layer is molasses, reaching a depth of 28.9 m. The soil deposit was considered to be fully saturated with water since the groundwater table was located at the surface. The relevant parameters used in this study were extracted from existing studies or calculated according to the determination methods described in Section 2, as shown in Table 2. It is noted that Young's modulus of the Molasse layer provided by Ravera et al. (2020a) was in the range of 3000-7000 MPa, based on which the calculated shear modulus fell in the range of 1153.8 - 2692.3 MPa. The initial stiffness of skin friction and tip reaction of the load transfer in the Molasse layer were calculated according to the equations mentioned in section 2.5 and fell in the range of

318.2-742.5 MPa/m and 2176.5-5078.5 MPa/m, respectively. Therefore, this study conducted two kinds of simulations using the maximum and minimum values of the initial stiffness of skin friction and tip reaction estimated from the shear modulus. The four energy piles were subjected to a heating-passive cooling cycle during the test. In this study, the monitoring results of EP1 pile (see Fig.6a) during the heating phase were used to validate the proposed model. The temperature changes were 5, 10, 15, and 20 ℃, respectively. Additionally, an initial vertical mechanical load of 495 kN was calculated for the single pile tested by Rotta Loria and Laloui (2017). A contact stiffness calculated as 4450 MPa/m was considered. Besides, thermal stress means pile vertical stress induced by temperature changes only.

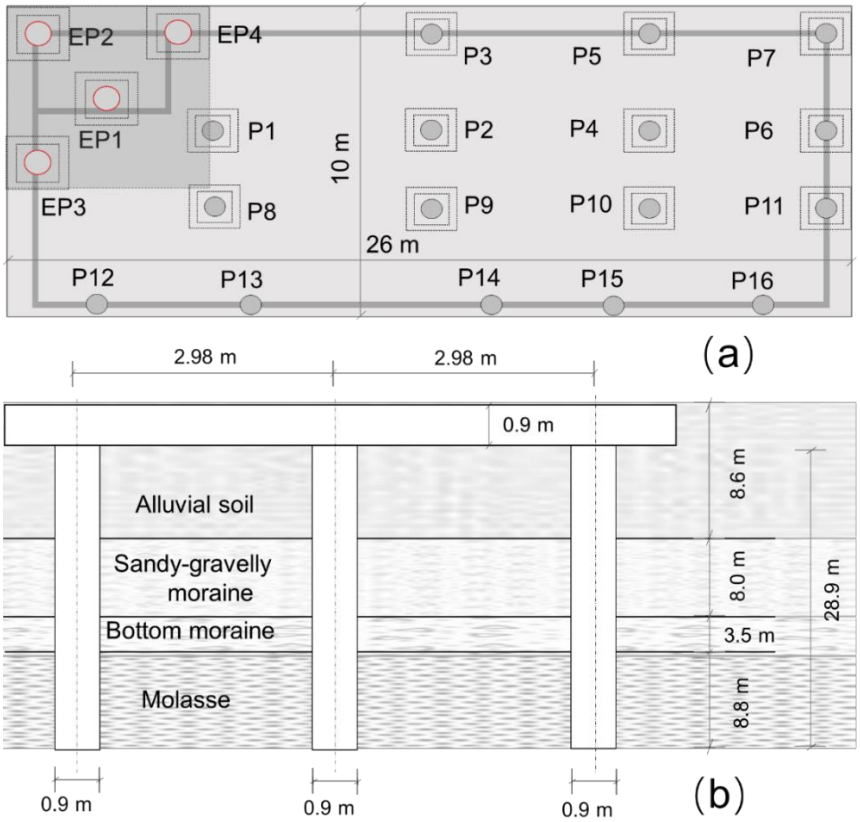

Fig.6 Schematic of (a) the energy pile foundation; (b) the soil stratigraphy (modified from Rotta Loria and Laloui 2017a, 2018a)

Table 2 Soil and pile parameters considered for modelling the field tests referring to (Rotta Loria and Laloui 2017b, Ravera et al. 2020a)

Variable \ Soil layer, z [m]	Alluvial soil [0.0, 8.6]	Sandy-gravelly moraine [8.6, 16.6]	Bottom moraine [16.6, 20.1]	Molasse [20.1, 28.9]	Pile tip [24, -]	Pile
Unit weight, γ_{sat} [kN/m^3]	19.8	19	19.8	25.5	-	25

Ultimate skin friction, τ_u $[kPa]$	7	17	28.9	50.8	-	-
Young's modulus, E $[MPa]$	5	84	90	3000-7000	-	28000
Shear modulus, $G_{soil}[MPa]$	2	30	32.1	1153.8 - 2692.3	-	-
Friction angle, φ [∘]	30	23	27	35	-	-
Initial stiffness of skin friction, $G_{max}[MPa/m]$	0.6	8.3	8.9	318.2 - 742.5	-	-
Ultimate tip resistance, q_b $[MPa]$	-	-	-	-	15.8	-
Initial stiffness of tip reaction, $G_{pmax}[MPa/m]$	-	-	-	-	2176.5-5078.5	-
Thermal dilation coefficient, α_s $(\mu\varepsilon/℃)$	-	-	-	-	-	10

Fig. 7 shows the comparison between experimentally observed and computed thermal vertical stress variations along the pile depth. It is noted that only the measured thermal stress along the pile depth of 4-28 m is presented for comparison because the heat exchange pipes were thermally insulated to a depth of 4 m below the pile heads to eliminate the effects of the climatic conditions on the test results and the temperature changes imposed to the piles in the present simulations were the mean values of the piles at a depth of 4-28 m recorded during the thermal operation (Rotta Loria and Laloui 2017b). It can be seen that the simulated results match well with the experimental results, especially in the lower temperature change operation (ΔT = 5 and 10 ℃). An increasing difference between the experimental and simulated values of the pile in the molasse layer is found under the higher thermal loads of ΔT = 15 and 20 ℃. The reason may be attributed to the fact that in the molasse layer, the present method is incapable of capturing the stress redistributions of the pile well under the condition that thermally induced deformation of the soil is more pronounced than that of the piles because the load transfer method used in this study is suitable for the case where the thermally induced deformations of piles govern the performance of energy piles. Similar phenomena and explanations can also be found in studies of Ravera et al.(2020a) and Rotta Loria et al.(2020b). Besides, the simulated results of the model proposed by Ravera et al.(2020a) are also shown for comparison purposes. It can be found that the present model does not need to use experiments or numerical simulations to determine the calculation parameters such as displacement factors and can achieve the same good calculation results as the model of Ravera et al.(2020a). The excellent

435 agreement between the simulated and experimental values of the current model and the
436 calculated values of other models shows the accuracy of the current model and its promising
437 potential for simulating thermomechanical responses of an energy pile group.

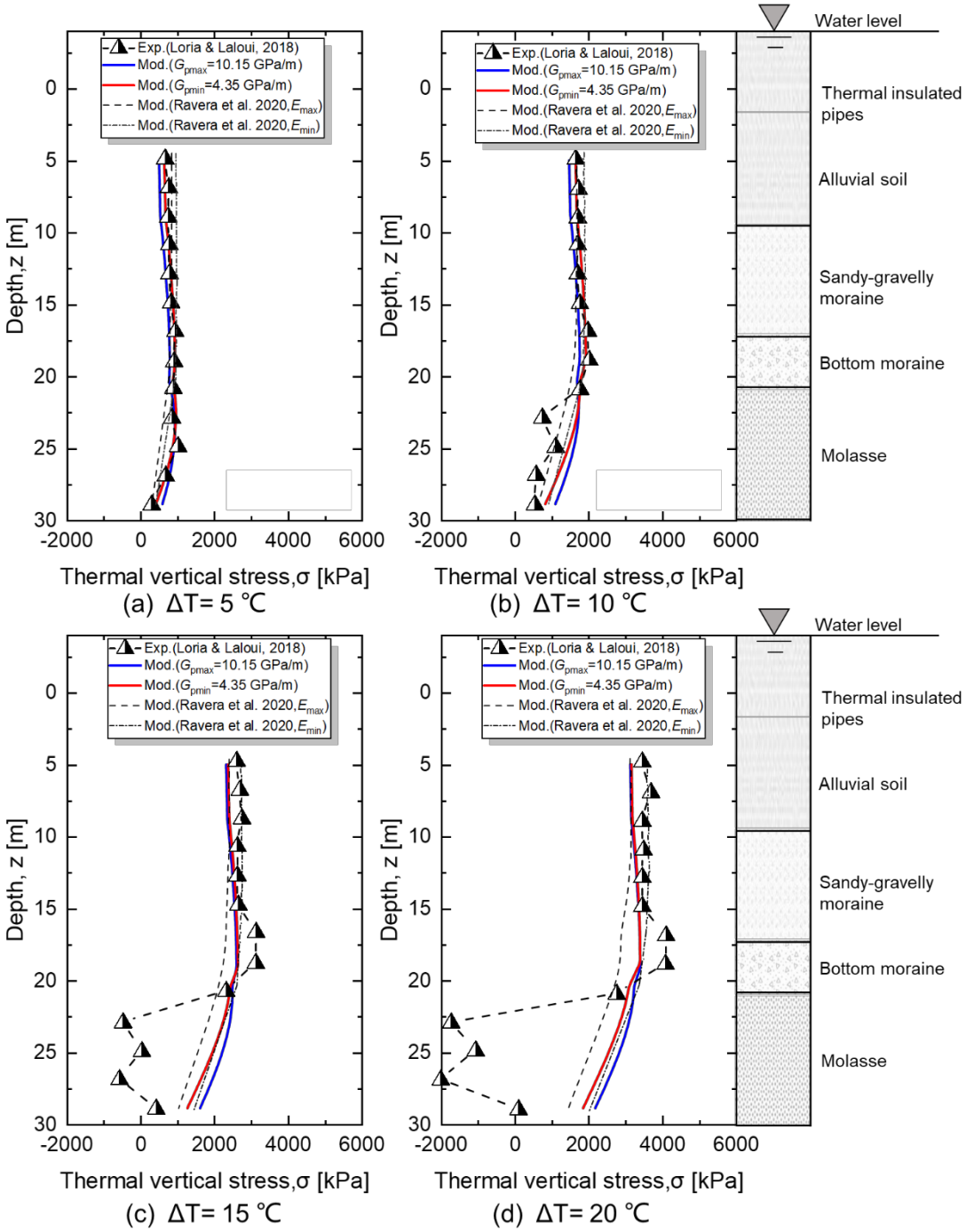

438
439 **Fig. 7** Comparison between experimentally observed and computed thermal vertical stresses
440 variations. (a) ΔT=5℃; (b) ΔT=10℃; (c) ΔT=15℃; (d) ΔT=20℃

441 **3.3 FE simulations of energy pile groups**

442 Saggu and Chakraborty (2016) conducted numerical studies of energy pile groups with

443 spacings of 2.5 and 4 m using the finite element software *Abaqus*. In these studies, the pile
444 group size was 3×2, and the slab was considered to be composed of the same concrete as the
445 pile. The slabs were 15.5 m long, 1.2 m thick, and 12.9 m wide. All piles, 20 m long and 1m in
446 diameter, were wished into a single layer of dry Ottawa sand. During the simulations, an axial
447 load of 6000 kN was continuously applied to the slab, and all the piles were first heated and
448 then recovered. The temperature changes were 21 and 2.8 ℃ at the heating and recovery ends,
449 respectively. The parameters used in this study are listed in Table 3. A contact stiffness
450 calculated as 401.7 MPa/m was considered in the study.

451 **Table 3** Soil and pile parameters considered in the present study referring to Saggu &
452 Chakraborty (2016)

Variable \ Soil layer, z [m]	Ottawa sand [0, 20]	Pile tip [24, -]	Pile
Unit weight, $\gamma\ [kN/m^3]$	18	-	25
Ultimate skin friction, $\tau_u\ [kPa]$	31.6	-	-
Shear modulus, $G_{soil}[MPa]$	32.6	-	-
Friction angle, $\varphi\ [\circ]$	32	-	-
Initial stiffness of skin friction, $G_{max}[MPa/m]$	16.2	-	-
Ultimate tip resistance, $q_b\ [MPa]$	-	8.3	-
Initial stiffness of tip reaction, $G_{pmax}[MPa/m]$	-	118.6	-
Young's modulus, $E_P\ (GPa)$	-	-	33.7
Thermal dilation coefficient, $\alpha_s\ (\mu\varepsilon/℃)$	-	-	10

453 Fig.8 shows the FE simulated and modeled pile axial stresses, referring to Saggu and
454 Chakraborty (2016). Fig.9(a), (b), and (c) show the axial stress in piles with 2.5 m center-to-
455 center spacing. Close agreement was observed between the FE simulations and the results of
456 the present model. Under mechanical loading, the pile stress decreases with depth. The axial
457 stress of the pile significantly increased when the pile temperature change reached 21 ℃. The
458 vertical stress at the end of the recovery phase was slightly higher than that under mechanical
459 loading, because the pile did not return to the initial temperature. An interesting phenomenon
460 is that the corner piles show a more significant thermal stress than the central piles because of
461 the interaction effects, which is in agreement with previous studies (Jeong et al. 2014,
462 Suryatriyastuti et al. 2016). A similar phenomenon can be observed in Fig.9(d), (e), and (f) for
463 the piles with 4.0 m center-to-center spacing.

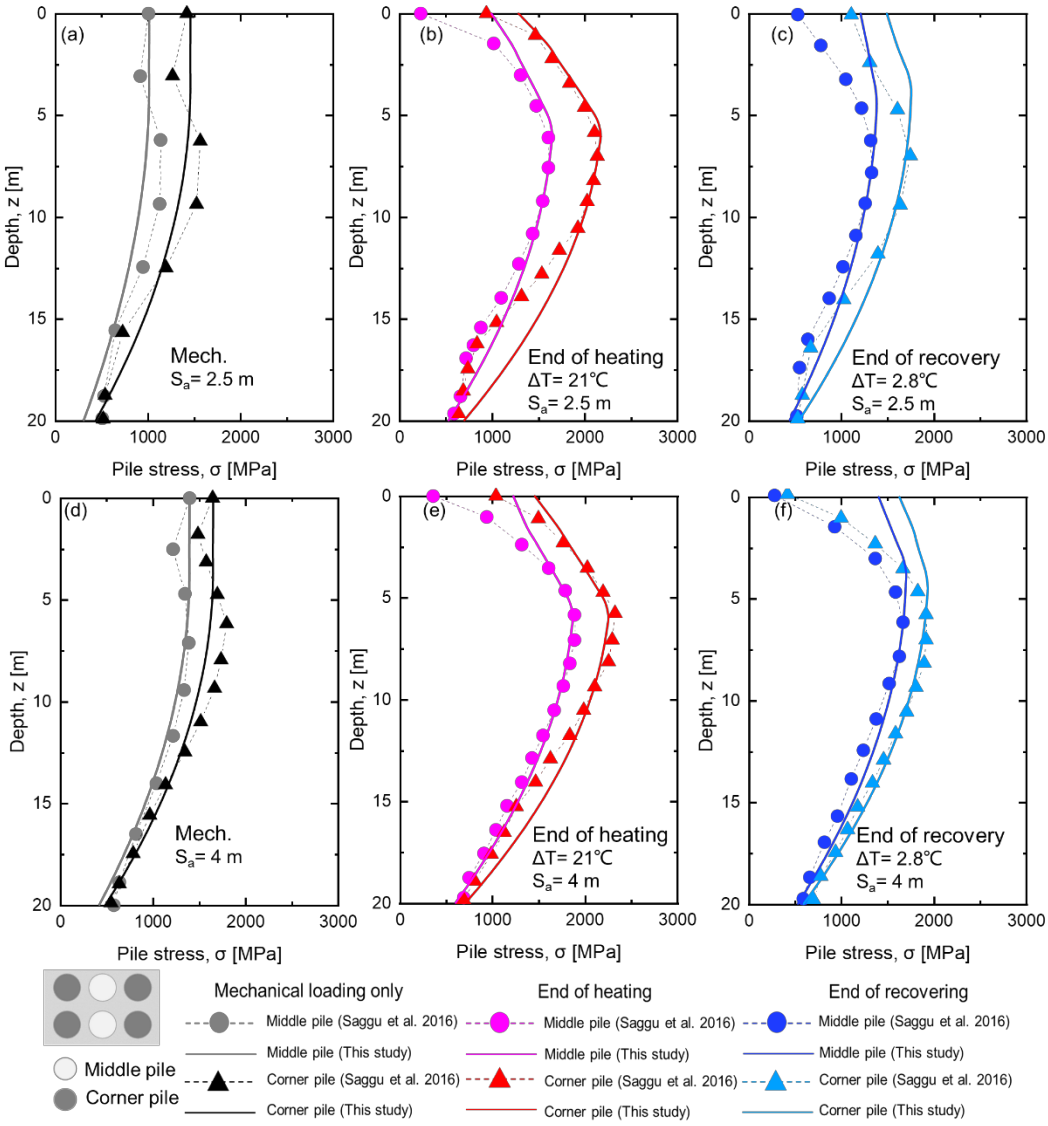

Fig. 8 FE simulated and modeled pile axial stresses referring to Saggu & Chakraborty(2016). (a), (b), and (c) are the axial stresses in pile with 2.5 m center-to-center spacing; (d), (e), and (f) are the axial stresses in pile with 4.0 m center-to-center spacing

Furthermore, finite element simulations of Rotta Loria and Laloui (2016) were employed for comparison with the simulations of the proposed model in this study to investigate the 'sheltering-reinforcing' effect in an energy pile group. The piles in the group had a length of 10 m and a diameter of 1 m. Young's modulus and Poisson's ratio of the piles were 30 GPa and 0.25, respectively. The thermal dilation coefficient of the piles was 10 $\mu\varepsilon/$℃. The piles were sited into homogeneous sand with a shear modulus of 30 MPa and a Poisson's ratio of 0.3. The temperature change is 10 ℃ during the simulations. The contact stiffness was considered to be zero since the pile head could move freely.

Rotta Loria and Laloui (2016) defined the displacement ratio to analyze the displacement characterizing energy pile group. The displacement ratio is expressed as:

$$R_d = \frac{\text{Average displacement of group}}{\text{Displacement of single pile under the same average load}} \tag{31}$$

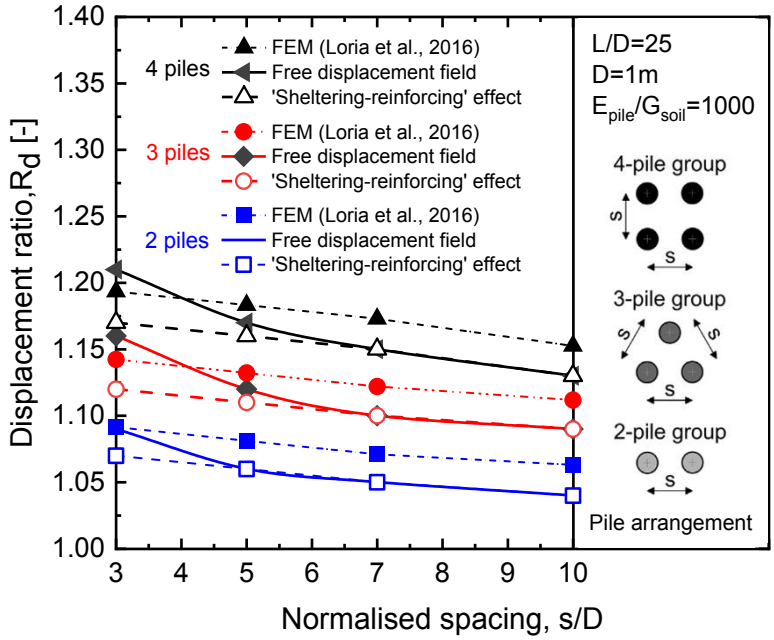

Fig. 9 Displacement ratio under the different pile spacings

Fig.9 shows the displacement ratio for various pile groups under different pile spacings. It can be seen that there is good agreement between the results of the finite element simulation and the results obtained by the present method with and without the 'sheltering-reinforcing' effect in the group. The difference between the results without and with consideration of the 'sheltering-reinforcing' effect tend to disappear when s/D is larger and the convergence is delayed if the number of piles increases. The displacement ratio obtained by the finite element simulation is the largest, and the results without and with consideration of the 'sheltering-reinforcing' effect are smaller and smallest, respectively. The possible reasons, similar to those discussed by Liu et al. (2022), are as follows:

(i) The nonlinear interaction of the pile-soil interface is not considered in the finite element simulations of Rotta Loria and Laloui (2016). Thus, when the pile is subjected to the thermal load, the pile and soil will deform together, and there is

493 no relative slip between them. However, the nonlinear pile-soil interaction is
494 considered in the proposed model, which means there will be a relative slip
495 between the pile and soil. The shaft resistance induced by surrounding soil will
496 hinder the upward expansion of the pile. Therefore, the displacement ratio
497 obtained by the finite element simulation is greater than that obtained by the model
498 proposed in this study.

499 (ii) Even though the nonlinear mechanical properties of the interface have been
500 considered, the calculation without considering the 'sheltering-reinforcing' effect
501 would overestimate the displacement ratio of the pile.

502 Besides, the displacement ratio obtained in the free displacement field increases significantly
503 when s/D=3. The reason may be that the shear displacement of the surrounding soil in the free
504 displacement field varies according to a non-linear decreasing function with pile spacing and
505 increases rapidly at smaller pile spacings (Wang et al., 2016). The comparison results show the
506 importance of considering the 'sheltering-reinforcing' effect in estimating the energy pile group
507 response and the relevance of the model proposed in the present study.

508 ## 4. Parametric study

509 This section aims to study the influence of the pile-slab-soil interaction, pile spacing, pile
510 position and number in a group using the present load transfer model. To this end, a series of
511 simulations was conducted using the parameters listed in Table 4.

512 **Table 4** Soil and pile parameters considered in the present study

Variable	Value
Length, $L[m]$	25
Pile diameter, $D[m]$	1
Young's modulus of piles, E_P (GPa)	30
Unit weight, γ $[kN/m^3]$	19.8
Friction angle, φ [∘]	33
Thermal dilation coefficient of piles, α_s $(\mu\varepsilon/℃)$	10
Mechanical load, P $[kN]$	3000
Ultimate skin friction, τ_u $[kPa]$	40.1
Initial stiffness of skin friction, $G_{s,max}[MPa/m]$	30
Ultimate tip resistance, σ_{up} $[MPa]$	10
Initial stiffness of tip reaction, $G_{pmax}[MPa/m]$	1500

4.1 Effect of the pile-slab-soil interaction

To study the effect of the pile-slab-soil interaction on the thermomechanical behavior of an energy pile group, a 2×2 pile group and an isolated pile were modeled. The pile-to-pile spacing of the group was three times the pile diameter. The parameters used in simulations are shown in Table 4. The piles were subjected to temperature changes of 10 and 30 ℃. Contact stiffness values of 0, 1, 3, 5, and 7 GPa/m were used in simulations. Fig.10 shows the effect of the contact stiffness on the thermal vertical stress of the pile. It can be observed that more thermal stress was induced as the contact stiffness increased. The thermal stress generated at the pile head of the pile group was slightly larger owing to the pile-slab-soil interaction. Fig.11 shows the effect of the contact stiffness on the maximum thermal vertical stress in the pile. It can be found that the maximum thermal stress in the pile in the group under the same contact stiffness was smaller than that of the isolated pile. This phenomenon has also been observed in previous studies (Suryatriyastuti et al. 2016, Ravera et al. 2020a).

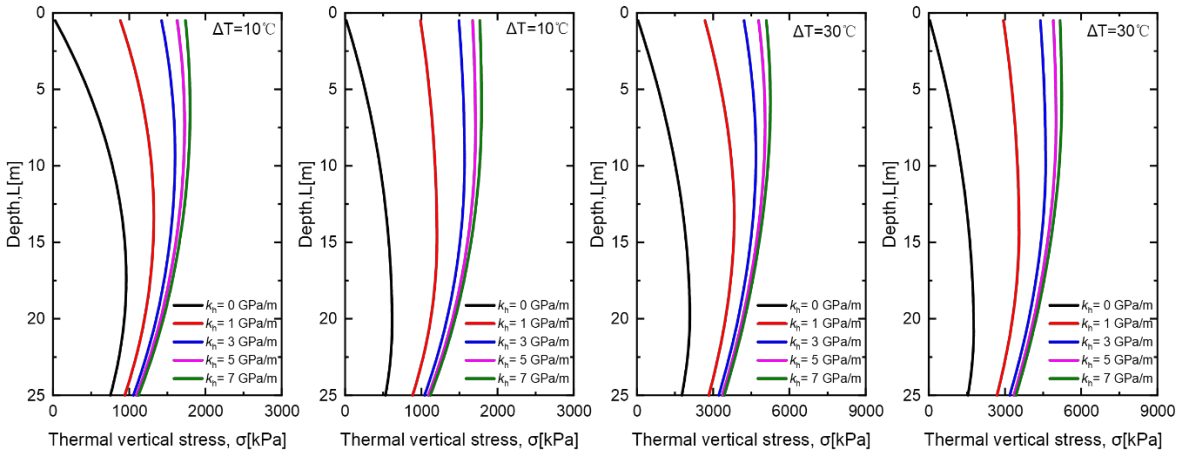

Fig. 10 Effect of contact stiffness on the thermal vertical stress of the pile. (a) and (b) are the thermal vertical stress under a temperature change of 10 ℃ of an isolated pile and a pile in a 2×2 group, respectively; (c) and (d) are the thermal vertical stress under a temperature change of 30 ℃ of an isolated pile and a pile in a 2×2 group

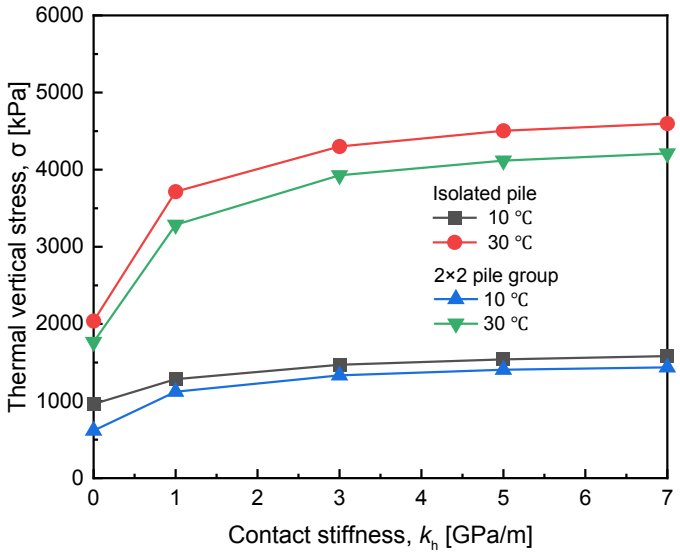

Fig. 11 Effect of contact stiffness on maximum thermal vertical stress of the pile

The thermally induced downward displacement of the pile under different levels of pile-slab-soil interaction is compared in Fig.12. According to the study of Najma and Sharma (2021), the location of the NP (i.e., thermally induced displacement equal to zero) approaches the pile head with greater pile head constraint, which explains why the position of NP gradually moves upward as the contact stiffness increases. It is also observed that the absolute values of the pile head and end displacements decreased and increased, respectively, as the contact stiffness increased. Additionally, the NP of the pile group was lower than that of the isolated pile under the same constraint conditions. Fig.13 presents the effect of the contact stiffness on the absolute value of the maximum thermal vertical displacement of the pile. Compared with the isolated piles, the pile group had larger thermally induced displacements under the same constraints; however, this difference became insignificant as the temperature change increased.

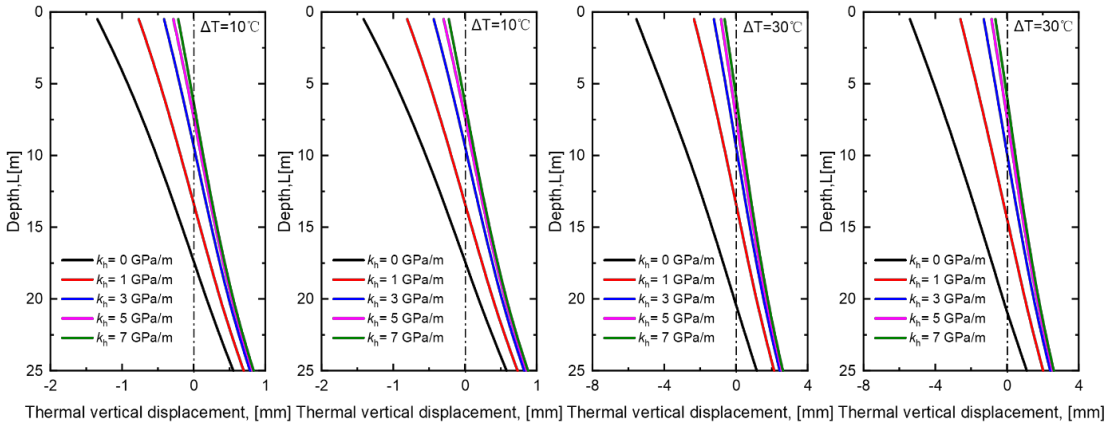

Fig. 12 Effect of the contact stiffness on thermal vertical displacement of the pile. (a) and (b) are the thermal vertical displacement under a temperature change of 10 ℃ of an isolated pile and a pile in a 2×2 group; (c) and (d) are the thermal vertical displacement under a temperature change of 30 ℃ of an isolated pile and a pile in a 2×2 group

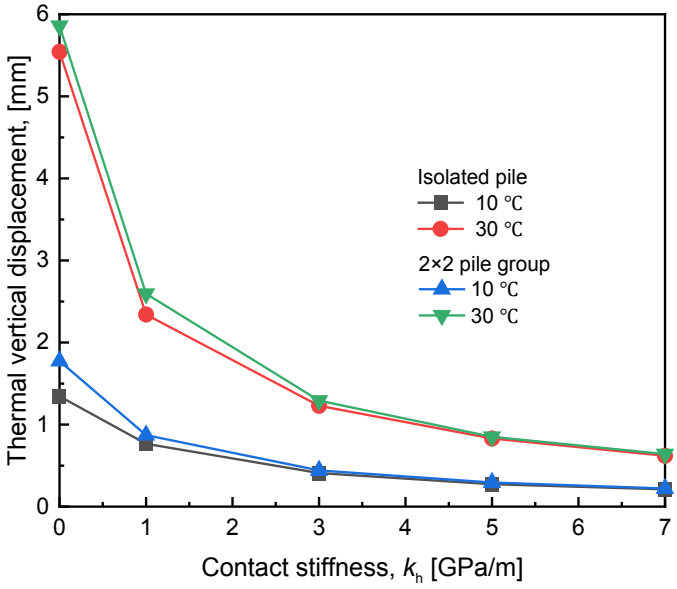

Fig. 13 Effect of the contact stiffness on the absolute value of maximum thermal vertical displacement of the pile

4.2 Effect of the pile spacing

Section 3.3 investigated the effect of pile spacing on a group with 2, 3 and 4 piles. In this section, the study was extended to a 5×5 pile group. The parameters used in the simulation are shown in Table 4. The pile-to-pile spacing of the group was three times the pile diameter. During the simulation, all the group piles were energy piles and subjected to a temperature change of 30 ℃. Besides, contact stiffness equal to zero was considered. Fig.14 shows the vertical thermal

displacement of the pile head subjected to different spacings. It can be observed that the thermal displacements decreased with increasing pile spacing, which is consistent with the results of Jeong et al. (2014) and Rotta Loria et al. (2016). This may be because an increase in pile spacing weakens the pile interactions within the group. The mechanism was discussed in detail in a study by Rotta Loria et al.(2016) on the interaction factor of energy-pile groups. In addition, the comparison results with and without considering the 'sheltering-reinforcing' effect, shown in Fig.14, further indicate the advantage of the present method in the analysis of the response of the energy pile group.

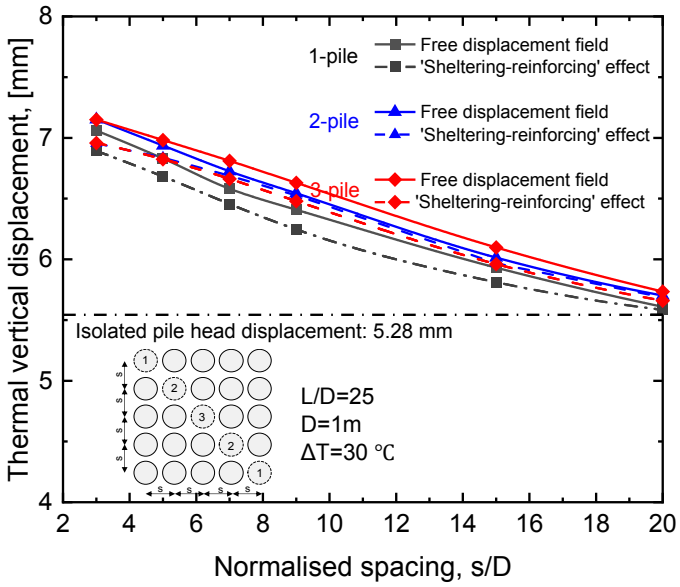

Fig. 14 Thermal displacement of the pile head under different pile spacing

4.3 Effect of pile position in a group

This section aims to study the effect of the pile position in a 3×3 group on the thermomechanical response. The pile-to-pile spacing of the group was three times the pile diameter. During the simulation, all the group piles were energy piles and subjected to a temperature change of 10 and 30 ℃. Besides, contact stiffness equal to zero was considered. Fig.15 shows a comparison of the profiles of the vertical thermal stress and displacement for the corner, edge, and center energy piles. For the sake of clarity, the effect of pile position in the group on the maximum thermal vertical stress and displacement of the pile under

temperature changes of 10 and 30 ℃ is summarized in Fig.16. It can be observed that the maximum and minimum thermal stresses occur at the corner and center piles, respectively, whereas the minimum and maximum thermal displacements occur at the corner and center piles, respectively. The position of the NP for the corner and center piles are the highest and lowest, respectively, which means that the corner piles are more constrained than the center piles in the group. The results of the energy pile group subjected to thermomechanical loads were in accordance with those of the energy pile group conducted by Ravera et al. (2020a) and the conventional pile group performed by Comodromos et al.(2016).

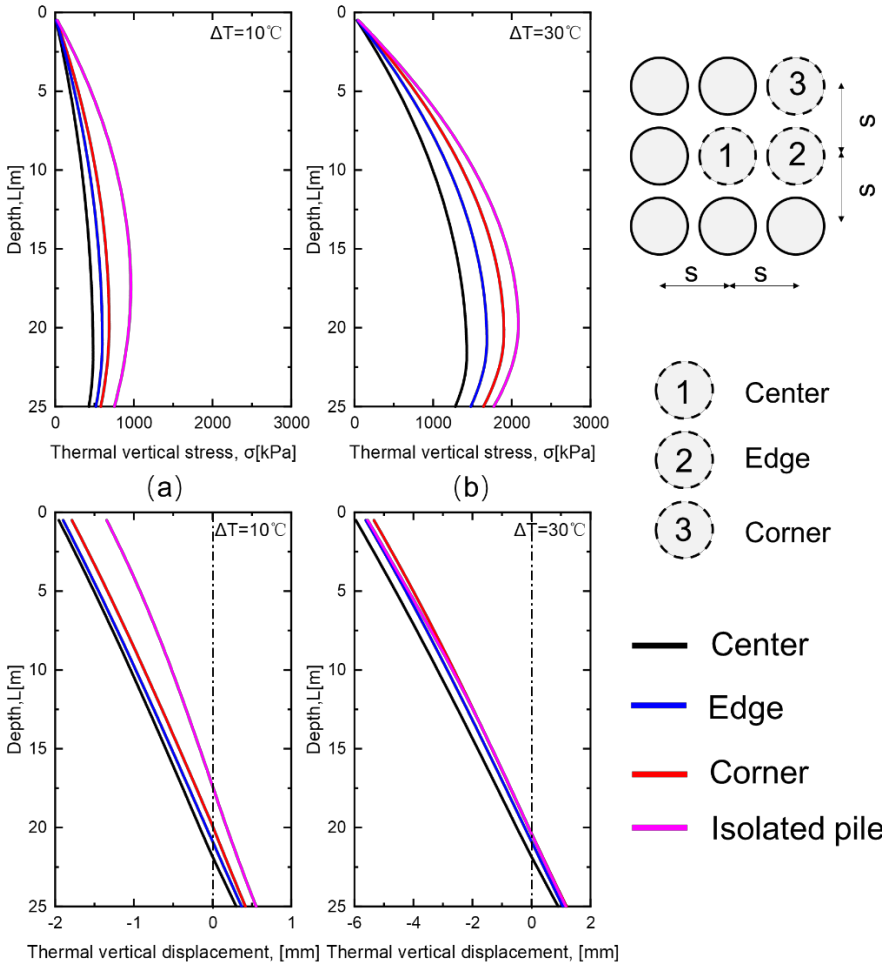

Fig. 15 Effect of pile arrangement in a group. Thermal vertical stress of the pile under (a) ΔT=10 ℃and (b) ΔT=30 ℃; thermal vertical displacement of the pile under (c) ΔT=10 ℃; (d) ΔT=30 ℃

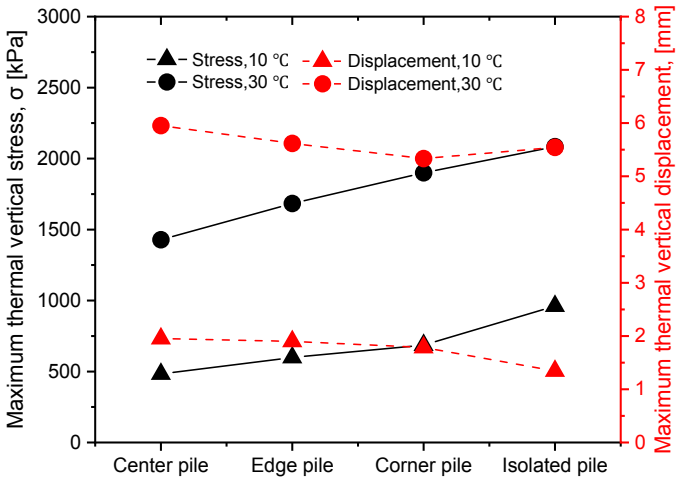

Fig. 16 Effect of pile position in the group on the maximum thermal vertical stress and the absolute value of the displacement of the pile under temperature changes of 10 and 30 ℃

4.4 Effect of the number of piles in the group

This section aims to study the effect of the number of piles in the group on the thermomechanical response. The pile-to-pile spacing of the group was three times the pile diameter. During the simulation, all the group piles were energy piles and subjected to a temperature change of 10 and 30 ℃. Besides, contact stiffness equal to zero was considered in the present case. Fig.17 presents the effect of the number of piles in the group, in which the thermally induced stress and displacement of an isolated pile (1×1) and 2×2, 3×3, 4×4, and 5×5 pile groups were modeled and compared. For the sake of clarity, the effect of the number of piles in the group on the maximum thermal vertical stress and the absolute values of the displacement of the pile under temperature change of 10 and 30 ℃ is summarized in Fig.18. The difference between thermal stresses in the pile group and the isolated pile decreased as the temperature increased. However, the pile head displacement increased with the number of piles. These results are consistent with those found by experimental and numerical studies(Rotta Loria and Laloui 2017b, Ravera et al. 2020a, Fang et al. 2022) and validate the applicability of the present method to simulate the interactions and group effects of energy piles.

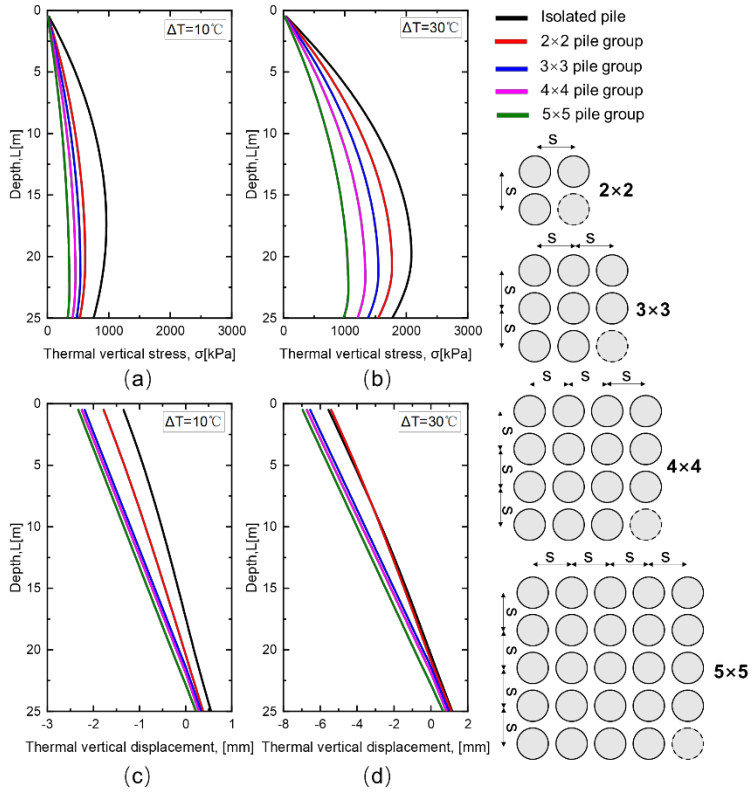

606

607 **Fig. 17** Effect of the number of piles in the group. Thermal vertical stress of the pile under (a)
608 ΔT=10 ℃ and (b) ΔT=30 ℃; thermal vertical displacement of the pile under (c) ΔT=10 ℃; (d)
609 ΔT=30 ℃.

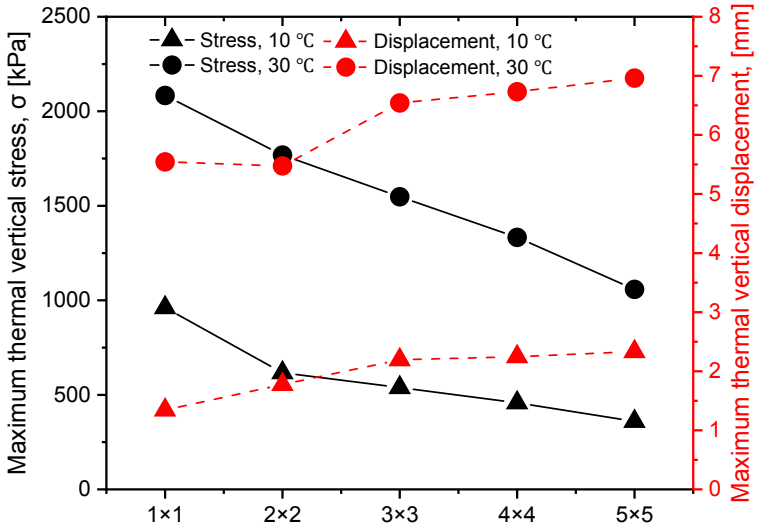

610

611 **Fig. 18** Effect of the number of the pile in the group on the maximum thermal vertical stress
612 and the absolute value of the displacement of the pile under temperature changes of 10 and
613 30 ℃.

614 **5. Discussion**

615 In this study, we proposed an experimentally validated load transfer model that considers

616 the ‘sheltering-reinforcing’ effect for the thermomechanical analysis of energy pile groups. The
617 proposed method modeled two well-documented full-scale field tests and two finite-element
618 simulation cases. The comparison results showed that the proposed method could capture
619 several essential aspects of the energy pile group, including thermally induced strain, stress,
620 displacement, and group effects. Also, we conducted a parametric analysis to evaluate the
621 effects of relevant parameters on the thermomechanical behavior of the energy pile group.

622 Recently, several methods considering pile-pile interactions have been developed for the
623 thermomechanical analysis of energy pile groups. For example, Rotta Loria and Laloui (2018)
624 proposed an analytical model to analyze the vertical displacement and the increased
625 deformation of energy pile groups subjected to thermal loads more comprehensively by
626 defining a pile-soil-pile interaction factor. Iodice et al. (2021) provided a unified methodology
627 involving a novel explicit formula for evaluating the maximum thermally induced axial load by
628 establishing the effect of the actual restraint condition at the pile head as a function of the
629 stiffness ratio between the inactive and the active pile subgroups. Nevertheless, the present
630 study is different from the above studies. First, the present study aims to provide an
631 experimentally validated simple load transfer model that considers the ‘sheltering-reinforcing’
632 effects for thermomechanical analysis of energy pile groups. The model can estimate all the
633 thermomechanical behavior of energy pile groups involving vertical displacement, strain, stress,
634 side friction, and group effects. This aim is very different from Rotta Loria and Laloui (2018)
635 study, which mainly focuses on estimating the vertical displacement of the energy pile group.
636 Furthermore, this study developed the load transfer method for the single energy pile under
637 thermomechanical loading by considering the pile-pile interaction in the group to make it
638 suitable for the thermomechanical behavior of energy pile groups. This is different from the

study of Iodice et al. (2021) because they fulfilled their aim by analyzing numerical simulation results and proposed the design procedure by using analytical solutions, which can be worked out to obtain explicit formulae for the direct computation of axial force in a multilayer soil. Their practical method is more geared toward calculating the thermomechanical responses of single energy piles. Second, The present study considers both nonlinear pile-soil interaction and elastic deformation of the surrounding soil. The surrounding soil is divided into disturbed and undisturbed zones. The soil in the disturbed zone is a skinny layer of soil on the soil/pile interface. The nonlinearity of the pile-soil interaction was concentrated in this interface. The area outside the interface is the undisturbed zone. Because this zone is subjected to a relatively low stress change, the stress-strain behavior of the soil is mainly elastic. The pile-soil-pile interaction in the pile group is considered linearly elastic and suitable for the principle of superposition. The advantage of this approach is that it can consider the relative slip between piles and soil for the single pile and the interaction between piles-soil-pile in pile groups. Thus, the consideration of pile-soil-pile interaction in the present study is very different from the two studies(Rotta Loria & Laloui, 2018; Iodice et al., 2021).

One of basic assumptions of the simple load transfer method is that the mechanical behavior of the energy pile is governed by thermally induced pile axial deformation. Thus, the radial deformation induced by thermal loading is not considered in the present study. There is controversy about whether the influence of radial deformation of energy piles on the response of piles can be ignored in the study of simplified analysis methods. Wang et al. (2015) and Faizal et al.(2018) showed that axial thermal strains were more restricted to thermal expansion than radial thermal strains, which indicated that the radial thermal strains are closer to that of the pile in free thermal expansion. On the contrary, the study by Mimouni and Laloui (2015) showed that the radial thermal strains of the pile were much lower than the free thermal strains,

663 indicating that stiffer soils provided higher restriction to radial thermal strains than the case
664 reported by Wang et al. (2015) and Faizal et al. (2018). It suggests that building loads could
665 affect the development of radial thermal strains along the pile length. Saggu et al. (2015)
666 observed that the radial strains induced in a pile due to thermo-mechanical loading are higher
667 than that induced due to only mechanical loading. Elzeiny & Suleimam (2021) pointed out that
668 the horizontal pressure decreased by 2~5 kPa when colling the pile, which corresponds quite
669 well with the average stress associated with the measured reduction in pull-out capacity.
670 Bourne-Webb et al. (2022) conducted numerical simulations and comprehensively investigated
671 the problem. They reported that the horizontal stress changes induced by thermal loading have
672 significant potential effects on the thermomechanical behavior of energy piles. The effects
673 depend on the margin concerning the initial mobilization of the shaft resistance by the
674 mechanical load. In summary, the studies mentioned above suggested that the horizontal
675 thermally induced contact stresses would significantly influence the thermomechanical
676 behavior of energy piles because of the radial expansion and contraction of the pile under
677 heating and cooling.

678 However, these require a confirmation from field tests under building loads representing
679 actual boundary conditions. It is noted that the existing studies have different opinions. Olgun
680 et al. (2014) reported that radial contact pressures typically increase less than 15 kPa, which
681 cannot fully explain the shaft resistance observed in heating tests. They thought that the increase
682 of heat exchanger pile capacity in response to heating, observed in several small-scale
683 laboratory studies, cannot be directly attributed to the increase of contact pressure at the soil/pile
684 interface. Faizal et al. (2019) conducted a field test of the energy pile and found that the
685 magnitudes of the axial thermal strains were more constrained than the radial thermal strains at
686 all depths, leading to the development of axial and radial thermal stresses of up to –4.5 and –
687 0.015 MPa, respectively, for a change in average pile temperature of 24.1 ℃. The magnitudes
688 of the radial thermal stresses with changes in pile temperature were significantly lower than the
689 axial thermal stresses at all depths of the pile, indicating that the radial thermal expansion had

690 negligible effects on the development of axial thermal strains and stresses.

691 In some studies (Garbellini and Laloui 2019b, Iodice et al. 2020, 2023, Liu et al. 2022),
692 radial thermal effects are commonly considered relatively small compared to axial thermal
693 effects when predicting the axial thermal response of energy piles due to the low diameter-to-
694 length ratio of the pile. Some load transfer analysis methods have consistently validated and
695 predicted the axial thermal response of field- and centrifuge-scale energy piles by neglecting
696 the radial thermal effects (Knellwolf et al. 2011, Suryatriyastuti et al. 2014, Chen and
697 McCartney 2016, Luo and Hu 2019, Ravera et al. 2020a, Rotta Loria et al. 2020a, Hu and Luo
698 2020, Najma and Sharma 2021, Fei et al. 2022). Some numerical studies have also noted that
699 radial thermal stresses in the energy pile are significantly low compared to the axial thermal
700 stresses along the length of the pile (Ozudogru et al. 2015, Gawecka et al. 2017). Besides,
701 preliminary numerical and analytical studies on energy piles (Olgun et al. 2014, Zhou et al.
702 2016), along with a field study on an energy pile without end restraints (Faizal et al. 2018) have
703 used cavity expansion analyses to confirm that no significant changes in pile–soil contact
704 stresses are expected from the radial thermal expansion of the pile. However, these also need
705 validation at various depths of a field-scale energy pile under building loads.

706 In the present study, a simple load transfer method was proposed for analyzing the
707 thermomechanical behavior of energy pile groups. Therefore, the same assumption adopted by
708 some studies, including the load transfer method for the thermomechanical analysis of energy
709 pile and energy pile groups (Knellwolf et al. 2011, Suryatriyastuti et al. 2014, Chen and
710 McCartney 2016, Luo and Hu 2019, Ravera et al. 2020a, Rotta Loria et al. 2020a, Hu and Luo
711 2020, Najma and Sharma 2021, Fei et al. 2022) is employed to reduce the complexity of coupled
712 thermomechanical analysis.

713 During the development of the simple load transfer model, the shear radius proposed by
714 Randolph and Wroth (1978) is employed to calculate the initial stiffness of the pile-soil
715 interface, as shown in Eq.(30). The shear radius is affected by pile length, shear modulus and
716 Poisson's ratio of the soil. For the pile under pure mechanical loads, the shear radius has been

found to be almost constant with pile depth and more significant than the pile length. However, when the pile was subjected to thermal loads, Rotta Loria and Laloui (2018) conducted finite element simulations and found that the shear radius was not constant with the pile depth and smaller than the pile length. In this study, the calculation of the shear radius is considered in a simplified method. For the multi-layered soil, the shear modulus and Poisson's ratio of each soil layer are different, which means there will be different values of shear radius for each soil layer. Thus, the calculated shear radius varies with pile depth but remains unchanged within the same soil layer through this simplified method. The simplified method mentioned above for the homogeneous soil will fail to obtain a shear radius varying with depth. The calculated shear radius remains unchanged within all the pile depths because the shear modulus and Poisson's ratio of the soil keep constant, which may adversely affect the application of the proposed simple load transfer method for energy pile groups in the homogeneous soil. Furthermore, the shear radius is greater than the pile length under mechanical loads and generally smaller than the pile length under thermal loads (Randolph & Wroth, 1978; Rotta Loria & Laloui, 2018).

The proposed simple load transfer method for energy pile groups in the presented study can consider the combined thermal and mechanical loads. During the thermomechanical analysis, it is necessary to consider the shear radius induced by both mechanical and thermal loads. Therefore, the shear radius induced by mechanical loads is employed for the thermomechanical analysis because the radius induced by mechanical loads is much greater than that induced by thermal loads.

6. Conclusions

We proposed a simple load transfer method for the thermomechanical analysis of an energy pile group subjected to thermomechanical loads. The proposed method was validated using full-scale field tests and finite element numerical simulations. In addition, a numerical analysis was performed to evaluate the effects of relevant parameters on the thermomechanical behavior of energy pile groups. The main conclusions are as follows:

(1) The results obtained with the proposed method were compared with those from full-scale field tests and FE simulations. The comparison indicated that the proposed model could capture the thermal strain, stress, and displacement of the energy piles in the group under thermal and mechanical loads.

(2) Under the same constraints and thermal loads, the energy piles in the group exhibited less thermal stress and larger thermal displacement than the isolated piles. The difference in the thermal stress and displacement between the single energy pile and the energy pile in groups increases with the temperature change increases.

(3) The maximum and minimum thermal stresses occurred at the corner and center piles, whereas the minimum and maximum thermal displacements occurred at the corner and center piles, respectively. In addition, the thermal displacement decreased with increasing pile spacing.

(4) The thermal stress decreased as the number of energy piles in the group increased under the same thermal load. The difference between thermal stresses in the pile group and the isolated pile decreased as the temperature change increased.

Acknowledgments

This research was supported by the National Natural Science Foundation of China (Grant Nos. 52122805 and 52078103) and the China Scholarship Council (CSC) (Grant No. 202106060093).

List of notations

B_{slab}	width of the slab
c'	effective cohesion of the soil
D	diameter of the pile
E_P	Young's modulus of the pile
E_{soil}	Young's modulus of the soil
G	shear modulus of the soil
$G_{\mathrm{s,max}}$	initial stiffness of the pile-soil interface
G_{pmax}	initial stiffness of the pile tip-soil interface
G_s	soil shear modulus
$G_{L/2}$	soil shear modulus at the middle of the pile
G_L	soil shear modulus at the tip of the pile

773 K_h contact stiffness between the pile head and slab
774 L length of the pile
775 L_{slab} length of the slab
776 N_q load capacity coefficients
777 N_c load capacity coefficients
778 P mechanical load applied to the pile head
779 p pile-soil relative displacement
780 p_0 relative pile-soil displacement corresponding to the stress reversal point
781 p_{p} pile-soil relative displacement of the pile tip
782 p_{p0} relative displacement of the pile tip and soil corresponding to the stress reverse point
783 r_0 pile radius
784 r_m shear influence radius
785 s elastic displacement of the surrounding soil
786 s_{i0} displacement of pile *i* induced by its own load
787 s_{ij} additional displacement caused by j pile under its own load
788 s_{aij} distance between the axes of two piles
789 s_{p} elastic displacement of the soil at the pile tip
790 u total shaft displacement at a certain pile depth
791 u_0 total pile shaft displacement corresponding to the shaft shear stress reversal point
792 α_s thermal dilation coefficient of the pile
793 Δs_{i0} displacement induced by the 'sheltering-reinforcing' effects of pile j
794 δ soil shear modulus ratio
795 δ_s friction angle of the pile-soil interface
796 η loading and unloading branching judgment factor
797 κ loading and unloading branching judgment factor
798 ν_{soil} Poisson's ratio of the soil
799 σ_{p} pile tip resistance
800 σ_{up} ultimate pile tip resistance
801 σ_{p0} pile tip resistance corresponding to the stress reversal point
802 σ'_{vb} effective vertical stress at the pile tip
803 σ'_z effective overburden pressure
804 τ pile shaft shear stress
805 τ_u ultimate shear stress
806 τ_0 pile shaft stress corresponding to the stress reverse point
807 φ_{s} friction angle of the soil
808 φ' effective friction angle of the pile tip soil

809 **Reference**

810 Arzanfudi, M.M., Al-Khoury, R., Sluys, L.J., and Schreppers, G.M.A. 2020. A thermo-hydro-
811 mechanical model for energy piles under cyclic thermal loading. Computers and
812 Geotechnics, **125**(July): 103560. Elsevier. doi:10.1016/j.compgeo.2020.103560.
813 Bourne-Webb, P.J., Amatya, B., Soga, K., Amis, T., Davidson, C., and Payne, P. 2009.
814 Energy pile test at Lambeth College, London: geotechnical and thermodynamic aspects
815 of pile response to heat cycles. Géotechnique, **59**(3): 237–248.
816 doi:10.1680/geot.2009.59.3.237.
817 Bourne-Webb, P.J., and Bodas Freitas, T.M. 2020. Thermally-activated piles and pile groups
818 under monotonic and cyclic thermal loading–A review. Renewable Energy, **147**: 2572–
819 2581. Elsevier Ltd. doi:10.1016/j.renene.2018.11.025.

Bourne-Webb, P.J., Lupattelli, A., Freitas, T.M.B., and Salciarini, D. 2022. The influence of initial shaft resistance mobilisation in the response of seasonally, thermally-activated pile foundations in granular media. Geomechanics for Energy and the Environment, **32**: 100299. Elsevier.

Caputo, V. 1984. Pile foundation analysis: a simple approach to nonlinerity effects. Rivista Italiana di Geotecnica, **18**(1): 32–51.

Chen, D., and McCartney, J.S. 2016. Parameters for Load Transfer Analysis of Energy Piles in Uniform Nonplastic Soils. International Journal of Geomechanics, **17**(7): 04016159. doi:10.1061/(asce)gm.1943-5622.0000873.

Chen, D., and McCartney, J.S. 2017. Parameters for Load Transfer Analysis of Energy Piles in Uniform Nonplastic Soils. International Journal of Geomechanics, **17**(7): 04016159. doi:10.1061/(ASCE)GM.1943-5622.0000873.

Comodromos, E.M., Papadopoulou, M.C., and Laloui, L. 2016. Contribution to the design methodologies of piled raft foundations under combined loadings. Canadian Geotechnical Journal, **53**(4): 559–577. doi:10.1139/cgj-2015-0251.

Cui, C., Meng, K., Xu, C., Liang, Z., Li, H., and Pei, H. 2021. Analytical solution for longitudinal vibration of a floating pile in saturated porous media based on a fictitious saturated soil pile model. Computers and Geotechnics, **131**: 103942. Elsevier. doi:10.1016/j.compgeo.2020.103942.

Elzeiny, R., and Suleiman, M.T. 2021. Pull-Out Response of a Laboratory-Scale Energy Pile Subjected to Cooling Cycles. Journal of Geotechnical and Geoenvironmental Engineering, **147**(7): 4021044. American Society of Civil Engineers.

Faizal, M., Bouazza, A., Haberfield, C., and McCartney, J.S. 2018. Axial and radial thermal responses of a field-scale energy pile under monotonic and cyclic temperature changes. Journal of Geotechnical and Geoenvironmental Engineering, **144**(10): 4018072. American Society of Civil Engineers.

Faizal, M., Bouazza, A., McCartney, J.S., and Haberfield, C. 2019. Axial and radial thermal responses of energy pile under six storey residential building. Canadian Geotechnical Journal, **56**(7): 1019–1033. doi:10.1139/cgj-2018-0246.

Fang, J., Kong, G., Meng, Y., Wang, L., and Yang, Q. 2020. Thermomechanical Behavior of Energy Piles and Interactions within Energy Pile–Raft Foundations. Journal of Geotechnical and Geoenvironmental Engineering, **146**(9): 04020079. doi:10.1061/(asce)gt.1943-5606.0002333.

Fang, J., Kong, G., and Yang, Q. 2022. Group Performance of Energy Piles under Cyclic and Variable Thermal Loading. Journal of Geotechnical and Geoenvironmental Engineering, **148**(8): 1–10. doi:10.1061/(ASCE)GT.1943-5606.0002840.

Fei, K., Ding, S.-J., and Qin, H.-Y. 2022. Analysis of energy pile groups subjected to non-uniform thermal loadings. Underground Space,. Tongji University. doi:10.1016/j.undsp.2022.05.003.

Fei, K., Zhu, Z.H., Shi, Y.H., and Zhou, Y. 2020. A simplified method for geotechnical analysis of energy pile groups. Yantu Lixue/Rock and Soil Mechanics, **41**(12): 3889–3898. doi:10.16285/j.rsm.2020.0313.

Frank, R. 1982. Estimation par les paramètres pressiométriques de l'enfoncement sous charge axiale de pieux forés dans des sols fins. Bull Liaison Lab Ponts Chauss, (119).

Garbellini, C., and Laloui, L. 2019a. Three-dimensional finite element analysis of piled rafts with energy piles. Computers and Geotechnics, **114**(February): 103115. Elsevier. doi:10.1016/j.compgeo.2019.103115.

Garbellini, C., and Laloui, L. 2019b. Thermal stress analysis of energy piles. Géotechnique,: 1–12. doi:10.1680/jgeot.19.p.208.

Gawecka, K.A., Taborda, D.M.G., Potts, D.M., Cui, W., Zdravković, L., and Haji Kasri, M.S. 2017. Numerical modelling of thermo-active piles in London Clay. Proceedings of the Institution of Civil Engineers-Geotechnical Engineering, **170**(3): 201–219. Thomas Telford Ltd.

Georgiadis, K., Skordas, D., Kamas, I., and Comodromos, E. 2020. Heating and cooling induced stresses and displacements in heat exchanger piles in sand. Renewable Energy, **147**: 2599–2617. Elsevier Ltd. doi:10.1016/j.renene.2018.11.078.

Guo, Y., Songyu1, L., Guozhu1, Z., and Le1, C. 2018. Investigation on the thermo-mechanical behavior of free constrained full-scale PHC energy pile in multi-layer strata. Chinese Journal of Rock Mechanics and Engineering, **38**.

Hu, B., and Luo, Z. 2020. Life-cycle probabilistic geotechnical model for energy piles. Renewable Energy, **147**: 741–750. Elsevier Ltd. doi:10.1016/j.renene.2019.09.022.

Iodice, C., Di Laora, R., and Mandolini, A. 2020. Analytical Solutions for Ultimate Limit State Design of Thermal Piles. Journal of Geotechnical and Geoenvironmental Engineering, **146**(5): 1–14. doi:10.1061/(ASCE)GT.1943-5606.0002204.

Iodice, C., Di Laora, R., and Mandolini, A. 2023. A practical method to design thermally stressed piles. Géotechnique, **73**(1): 30–43. doi:10.1680/jgeot.20.P.231.

Jeong, S., Lim, H., Lee, J.K., and Kim, J. 2014. Thermally induced mechanical response of energy piles in axially loaded pile groups. Applied Thermal Engineering, **71**(1): 608–615. Elsevier Ltd. doi:10.1016/j.applthermaleng.2014.07.007.

KALANTIDOU, A., TANG, A.M., PEREIRA, J.-M., and HASSEN, G. 2012. Preliminary study on the mechanical behaviour of heat exchanger pile in physical model. Géotechnique, **62**(11): 1047–1051. doi:10.1680/geot.11.T.013.

Kezdi，A. 1957. Bearing Capacity of Piles and Pile Groups. *In* Proceedings of 4th International Conference on Soil Mechanics and Foundation Engineering．. London. pp. 46–51.

Knellwolf, C., Peron, H., and Laloui, L. 2011. Geotechnical Analysis of Heat Exchanger Piles. Journal of Geotechnical and Geoenvironmental Engineering, **137**(10): 890–902. doi:10.1061/(ASCE)GT.1943-5606.0000513.

Kong, G., Fang, J., Huang, X., Liu, H., and Abuel-Naga, H. 2020. Thermal induced horizontal earth pressure changes of pipe energy piles under multiple heating cycles. Geomechanics for Energy and the Environment, (xxxx): 100228. Elsevier Ltd. doi:10.1016/j.gete.2020.100228.

Laloui, L., Nuth, M., and Vulliet, L. 2006. Experimental and numerical investigations of the behaviour of a heat exchanger pile. International Journal for Numerical and Analytical Methods in Geomechanics, **30**(8): 763–781. doi:10.1002/nag.499.

Lee, C.Y. 1993. Pile groups under negative skin friction. Journal of geotechnical engineering,

119(10): 1587–1600. American Society of Civil Engineers.
Lee, K.M., and Xiao, Z.R. 2001. A simplified nonlinear approach for pile group settlement analysis in multilayered soils. Canadian Geotechnical Journal, **38**(5): 1063–1080. NRC Research Press Ottawa, Canada. doi:http://cgj.nrc.ca.
Lin, Z.-Y., and Dai, Z.-H. 2014. Interaction coefficients method for calculating piles group settlements considering reinforcing and restraining effect.
Liu, S., Zhang, Q., Cui, W., Liu, G., and Liu, J. 2022. A simple method for analyzing thermomechanical response of an energy pile in a group. Geomechanics for Energy and the Environment, (xxxx): 100309. Elsevier Ltd. doi:10.1016/j.gete.2022.100309.
Luo, Z., and Hu, B. 2019. Probabilistic design model for energy piles considering soil spatial variability. Computers and Geotechnics, **108**(December 2018): 308–318. Elsevier. doi:10.1016/j.compgeo.2019.01.003.
Mimouni, T., and Laloui, L. 2015. Behaviour of a group of energy piles. Canadian Geotechnical Journal, **52**(12): 1913–1929. doi:10.1139/cgj-2014-0403.
Moradshahi, A., Faizal, M., Bouazza, A., and McCartney, J.S. 2020. Effect of nearby piles and soil properties on the thermal behaviour of a field-scale energy pile. Canadian Geotechnical Journal,: 1–41. doi:10.1139/cgj-2020-0353.
Murphy, K.D., McCartney, J.S., and Henry, K.S. 2015. Evaluation of thermo-mechanical and thermal behavior of full-scale energy foundations. Acta Geotechnica, **10**(2): 179–195. doi:10.1007/s11440-013-0298-4.
Mylonakis, G., and Gazetas, G. 1998. Settlement and additional internal forces of grouped piles in layered soil. Geotechnique, **48**(1): 55–72. Thomas Telford Ltd.
Najma, A., and Sharma, J. 2021. Incremental load transfer analysis of an energy pile under arbitrary mechanical and thermal loads. Geomechanics for Energy and the Environment, **28**: 100243. Elsevier Ltd. doi:10.1016/j.gete.2021.100243.
Ng, C.W.W., Farivar, A., Gomaa, S.M.M.H., Shakeel, M., and Jafarzadeh, F. 2021. Performance of elevated energy pile groups with different pile spacing in clay subjected to cyclic non-symmetrical thermal loading. Renewable Energy, **172**: 998–1012. doi:10.1016/j.renene.2021.03.108.
Ng, C.W.W., Gunawan, A., Shi, C., Ma, Q.J., and Liu, H.L. 2016. Centrifuge modelling of displacement and replacement energy piles constructed in saturated sand: a comparative study. Géotechnique Letters, **6**(1): 34–38. doi:10.1680/jgele.15.00119.
Ng, C.W.W., and Ma, Q.J. 2019. Energy pile group subjected to non-symmetrical cyclic thermal loading in centrifuge. Geotechnique Letters, **9**(3): 173–177. doi:10.1680/jgele.18.00161.
Ng, C.W.W., Shi, C., Gunawan, A., Laloui, L., and Liu, H.L. 2015. Centrifuge modelling of heating effects on energy pile performance in saturated sand. Canadian Geotechnical Journal, **52**(8): 1045–1057. doi:10.1139/cgj-2014-0301.
Nguyen, V.T., Wu, N., Gan, Y., Pereira, J.-M., and Tang, A.M. 2019. Long-term thermo-mechanical behaviour of energy piles in clay. Environmental Geotechnics, (2015): 1–12. doi:10.1680/jenge.17.00106.
Olgun, C.G., Ozudogru, T.Y., and Arson, C.F. 2014. Thermo-mechanical radial expansion of heat exchanger piles and possible effects on contact pressures at pile–soil interface. Géotechnique Letters, **4**(3): 170–178. doi:10.1680/geolett.14.00018.

950 Ozudogru, T.Y., Olgun, C.G., and Arson, C.F. 2015. Analysis of friction induced thermo-
951 mechanical stresses on a heat exchanger pile in isothermal soil. Geotechnical and
952 Geological Engineering, **33**: 357–371. Springer.
953 Pei, H., Song, H., Meng, F., and Liu, W. 2022a. Long-term thermomechanical displacement
954 prediction of energy piles using machine learning techniques. Renewable Energy, **195**:
955 620–636. Elsevier Ltd. doi:10.1016/j.renene.2022.06.057.
956 Pei, H., Song, H., Zhou, C., Yang, Q., and Xiao, D. 2022b. Cyclic t-z model for the long-term
957 thermomechanical analysis of energy piles. Canadian Geotechnical Journal,: 1–45.
958 doi:10.1139/cgj-2022-0011.
959 Rammal, D., Mroueh, H., and Burlon, S. 2018. Impact of thermal solicitations on the design
960 of energy piles. Renewable and Sustainable Energy Reviews, **92**(April): 111–120.
961 Elsevier Ltd. doi:10.1016/j.rser.2018.04.049.
962 Randolph, M.F. 1994. Design methods for pile groups and piled rafts. *In* International
963 conference on soil mechanics and foundation engineering. pp. 61–82.
964 Randolph, M.F., and Wroth, C.P. 1978. Analysis of Deformation of Vertically Loaded Piles.
965 Journal of the Geotechnical Engineering Division, **104**(12): 1465–1488. American
966 Society of Civil Engineers. doi:10.1061/AJGEB6.0000729.
967 Randolph, M.F., and Wroth, C.P. 1979. An analysis of the vertical deformation of pile groups.
968 Geotechnique, **29**(4): 423–439. Thomas Telford Ltd.
969 Ravera, E., Sutman, M., and Laloui, L. 2020a. Load Transfer Method for Energy Piles in a
970 Group with Pile-Soil-Slab-Pile Interaction. Journal of Geotechnical and
971 Geoenvironmental Engineering, **146**(6): 1–17. doi:10.1061/(ASCE)GT.1943-
972 5606.0002258.
973 Ravera, E., Sutman, M., and Laloui, L. 2020b. Analysis of the interaction factor method for
974 energy pile groups with slab. Computers and Geotechnics, **119**(February): 103294.
975 Elsevier. doi:10.1016/j.compgeo.2019.103294.
976 Rotta Loria, A.F., Catalá Oltra, J. V., and Laloui, L. 2020a. Equivalent pier analysis of full-
977 scale pile groups subjected to mechanical and thermal loads. Computers and
978 Geotechnics, **120**(July 2019): 103410. Elsevier. doi:10.1016/j.compgeo.2019.103410.
979 Rotta Loria, A.F., Catalá Oltra, J. V., and Laloui, L. 2020b. Equivalent pier analysis of full-
980 scale pile groups subjected to mechanical and thermal loads. Computers and
981 Geotechnics, **120**(July 2019): 103410. Elsevier. doi:10.1016/j.compgeo.2019.103410.
982 Rotta Loria, A.F., and Coulibaly, J.B. 2021. Thermally induced deformation of soils: A
983 critical overview of phenomena, challenges and opportunities. Geomechanics for Energy
984 and the Environment, **25**: 100193. Elsevier Ltd. doi:10.1016/j.gete.2020.100193.
985 Rotta Loria, A.F., and Laloui, L. 2016. The interaction factor method for energy pile groups.
986 Computers and Geotechnics, **80**: 121–137. The Authors.
987 doi:10.1016/j.compgeo.2016.07.002.
988 Rotta Loria, A.F., and Laloui, L. 2017a. The equivalent pier method for energy pile groups.
989 Geotechnique, **67**(8): 691–702. doi:10.1680/jgeot.16.P.139.
990 Rotta Loria, A.F., and Laloui, L. 2017b. Thermally induced group effects among energy piles.
991 Geotechnique, **67**(5): 374–393. doi:10.1680/jgeot.16.P.039.
992 Rotta Loria, A.F., and Laloui, L. 2018. Group action effects caused by various operating
993 energy piles. Geotechnique, **68**(9): 834–841. doi:10.1680/jgeot.17.P.213.

994 Rotta Loria, A.F., Vadrot, A., and Laloui, L. 2018. Analysis of the vertical displacement of
995 energy pile groups. Geomechanics for Energy and the Environment, **16**: 1–14. Elsevier
996 Ltd. doi:10.1016/j.gete.2018.04.001.
997 Saeidi Rashk Olia, A., Cossel, A.E., and Perić, D. 2022. Analytical Solutions for
998 Thermomechanical Soil–Structure Interaction in Single Semifloating Energy Piles
999 Embedded in a Layered Soil Profile. Journal of Geotechnical and Geoenvironmental
1000 Engineering, **148**(10): 4022080. American Society of Civil Engineers.
1001 Saggu, R., and Chakraborty, T. 2015. Cyclic Thermo-Mechanical Analysis of Energy Piles in
1002 Sand. Geotechnical and Geological Engineering, **33**(2): 321–342. doi:10.1007/s10706-
1003 014-9798-8.
1004 Saggu, R., and Chakraborty, T. 2016. Thermomechanical Response of Geothermal Energy
1005 Pile Groups in Sand. International Journal of Geomechanics, **16**(4): 04015100.
1006 doi:10.1061/(ASCE)GM.1943-5622.0000567.
1007 Seed, H.B., and Reese, L.C. 1957. The action of soft clay along friction piles. Transactions of
1008 the American Society of Civil Engineers, **122**(1): 731–754. American Society of Civil
1009 Engineers.
1010 Selvadurai, A.P.S. 2013. Elastic analysis of soil-foundation interaction. Elsevier.
1011 Song, H., and Pei, H. 2022. A Nonlinear Softening Load-Transfer Approach for the
1012 Thermomechanical Analysis of Energy Piles. International Journal of Geomechanics,
1013 **22**(5): 1–14. doi:10.1061/(ASCE)GM.1943-5622.0002358.
1014 Song, H., Pei, H., Xu, D., and Cui, C. 2020. Performance study of energy piles in different
1015 climatic conditions by using multi-sensor technologies. Measurement,: 107875.
1016 doi:https://doi.org/10.1016/j.measurement.2020.107875.
1017 Song, H., Pei, H., Zhou, C., Zou, D., and Cui, C. 2022. Calculation of the representative
1018 temperature change for the thermomechanical design of energy piles. Geomechanics for
1019 Energy and the Environment, **29**(xxxx): 100264. Elsevier Ltd.
1020 doi:10.1016/j.gete.2021.100264.
1021 Suryatriyastuti, M.E., Burlon, S., and Mroueh, H. 2016. On the understanding of cyclic
1022 interaction mechanisms in an energy pile group. International Journal for Numerical and
1023 Analytical Methods in Geomechanics, **40**(1): 3–24. doi:10.1002/nag.2382.
1024 Suryatriyastuti, M.E., Mroueh, H., and Burlon, S. 2012. Understanding the temperature-
1025 induced mechanical behaviour of energy pile foundations. Renewable and Sustainable
1026 Energy Reviews, **16**(5): 3344–3354. Elsevier Ltd. doi:10.1016/j.rser.2012.02.062.
1027 Suryatriyastuti, M.E., Mroueh, H., and Burlon, S. 2014. A load transfer approach for studying
1028 the cyclic behavior of thermo-active piles. Computers and Geotechnics, **55**: 378–391.
1029 Elsevier Ltd. doi:10.1016/j.compgeo.2013.09.021.
1030 Sutman, M., Brettmann, T., and Olgun, C.G. 2019a. Full-scale in-situ tests on energy piles:
1031 Head and base-restraining effects on the structural behaviour of three energy piles.
1032 Geomechanics for Energy and the Environment, **18**: 56–68. Elsevier Ltd.
1033 doi:10.1016/j.gete.2018.08.002.
1034 Sutman, M., Olgun, C.G., and Laloui, L. 2019b. Cyclic Load–Transfer Approach for the
1035 Analysis of Energy Piles. Journal of Geotechnical and Geoenvironmental Engineering,
1036 **145**(1): 04018101. doi:10.1061/(ASCE)GT.1943-5606.0001992.
1037 Sutman, M., Speranza, G., Ferrari, A., Larrey-Lassalle, P., and Laloui, L. 2020. Long-term

performance and life cycle assessment of energy piles in three different climatic conditions. Renewable Energy, **146**: 1177–1191. Elsevier Ltd. doi:10.1016/j.renene.2019.07.035.

Trochanis, A.M., Bielak, J., and Christiano, P. 1991. Three-dimensional nonlinear study of piles. Journal of Geotechnical Engineering, **117**(3): 429–447. American Society of Civil Engineers.

Wang, A.D., Wang, W.D., Huang, M.S., Wu, J.B., Sheil, B.B., and McCabe, B.A. 2016. Interaction factor for large pile groups. Géotechnique Letters, **6**(3): 234–240. doi:10.1680/jgele.16.00082.

Wang, B., Bouazza, A., Singh, R.M., Haberfield, C., Barry-Macaulay, D., and Baycan, S. 2015. Posttemperature Effects on Shaft Capacity of a Full-Scale Geothermal Energy Pile. Journal of Geotechnical and Geoenvironmental Engineering, **141**(4): 04014125. doi:10.1061/(ASCE)GT.1943-5606.0001266.

Wong, K.S., and Teh, C.I. 1995. Negative skin friction on piles in layered soil deposits. Journal of Geotechnical Engineering, **121**(6): 457–465. doi:10.1061/(ASCE)0733-9410(1995)121:6(457).

Wu, D., Liu, H., Kong, G., and Ng, C.W.W. 2020. Interactions of an Energy Pile with Several Traditional Piles in a Row. Journal of Geotechnical and Geoenvironmental Engineering, **146**(4): 1–9. doi:10.1061/(ASCE)GT.1943-5606.0002224.

Wu, D., Liu, H., Kong, G., and Rotta Loria, A.F. 2021. Thermo-mechanical behavior of a full-scale energy pile equipped with a spiral pipe configuration. Canadian Geotechnical Journal,: cgj-2020-0162. doi:10.1139/cgj-2020-0162.

Yavari, N., Tang, A.M., Pereira, J.-M., and Hassen, G. 2014. A simple method for numerical modelling of mechanical behaviour of an energy pile. Géotechnique Letters, **4**(2): 119–124. doi:10.1680/geolett.13.00053.

Yavari, N., Tang, A.M., Pereira, J.M., and Hassen, G. 2016a. Mechanical behaviour of a small-scale energy pile in saturated clay. Geotechnique, **66**(11): 878–887. doi:10.1680/jgeot.15.T.026.

Yavari, N., Tang, A.M., Pereira, J.M., and Hassen, G. 2016b. Effect of temperature on the shear strength of soils and the soil–structure interface. Canadian Geotechnical Journal, **53**(7): 1186–1194. doi:10.1139/cgj-2015-0355.

Yazdani, S., Helwany, S., and Olgun, G. 2019a. Experimental evaluation of shear strength of kaolin clay under cyclic and noncyclic thermal loading. Geotechnical Testing Journal, **42**(6): 1518–1548. doi:10.1520/GTJ20180020.

Yazdani, S., Helwany, S., and Olgun, G. 2019b. Investigation of Thermal Loading Effects on Shaft Resistance of Energy Pile Using Laboratory-Scale Model. Journal of Geotechnical and Geoenvironmental Engineering, **145**(9): 04019043. doi:10.1061/(ASCE)GT.1943-5606.0002088.

Zhang, Q., Liu, S., Zhang, S., Zhang, J., and Wang, K. 2016. Simplified non-linear approaches for response of a single pile and pile groups considering progressive deformation of pile–soil system. Soils and Foundations, **56**(3): 473–484. Elsevier. doi:10.1016/j.sandf.2016.04.013.

Zhou, H., Kong, G., Liu, H., Wu, Y., and Li, G. 2016. A novel cavity expansion-based analytical tool and its potential application for energy pile foundation. *In* Proceedings of

the 1st International Conference on Energy Geotechnics, ICEGT. pp. 359–365.